Paleoceanography and Paleoclimatology

RESEARCH ARTICLE
10.1029/2021PA004309

Key Points:

- New paired Baltic carbonate data set improves Ordovician ^{18}O- and ^{13}C-record
- The new data supports a Middle Ordovician sea surface temperature cooling
- Regional/intra-basinal consistency of oxygen isotope trends indicate primary nature of paleoenvironmental changes

Supporting Information:

Supporting Information may be found in the online version of this article.

Correspondence to:

C. M. Ø. Rasmussen,
c.macorum@sund.ku.dk

Citation:

Edward, O., Korte, C., Ullmann, C. V., Colmenar, J., Thibault, N., Bagnoli, G., et al. (2022). A Baltic perspective on the Early to early Late Ordovician $\delta^{13}C$ and $\delta^{18}O$ records and its paleoenvironmental significance. *Paleoceanography and Paleoclimatology*, *37*, e2021PA004309. https://doi.org/10.1029/2021PA004309

Received 20 MAY 2021
Accepted 15 FEB 2022

Author Contributions:

Conceptualization: Christoph Korte, Christian M. Ø. Rasmussen
Data curation: Oluwaseun Edward, Gabriella Bagnoli, Svend Stouge
Formal analysis: Oluwaseun Edward, Clemens V. Ullmann, Nicolas Thibault, Gabriella Bagnoli, Svend Stouge
Funding acquisition: Christian M. Ø. Rasmussen
Investigation: Oluwaseun Edward, Svend Stouge, Christian M. Ø. Rasmussen
Methodology: Oluwaseun Edward, Christoph Korte, Clemens V. Ullmann

A Baltic Perspective on the Early to Early Late Ordovician $\delta^{13}C$ and $\delta^{18}O$ Records and Its Paleoenvironmental Significance

Oluwaseun Edward[1,2], Christoph Korte[1], Clemens V. Ullmann[3], Jorge Colmenar[4], Nicolas Thibault[1], Gabriella Bagnoli[5], Svend Stouge[6], and Christian M. Ø. Rasmussen[7]

[1]Department of Geosciences and Natural Resource Management, University of Copenhagen, Copenhagen K, Denmark, [2]Institute of Earth Surface Dynamics, University of Lausanne, Lausanne, Switzerland, [3]Camborne School of Mines, College of Engineering, Mathematics and Physical Sciences, University of Exeter, Penryn Campus, Penryn, UK, [4]Instituto Geológico y Minero de España, Madrid, Spain, [5]Department of Earth Sciences, University of Pisa, Pisa, Italy, [6]Natural History Museum of Denmark, University of Copenhagen, Copenhagen K, Denmark, [7]GLOBE Institute, University of Copenhagen, Copenhagen K, Denmark

Abstract The current study presents new bed-by-bed brachiopod $\delta^{13}C$ and $\delta^{18}O$ records from Öland, Sweden, which together with previously published data from the East Baltic region, constitutes a high-resolution paired brachiopod and bulk rock carbon and oxygen isotope archive through the Lower to Upper Ordovician successions of Baltoscandia. This new data set refines the temporal control on the global Ordovician $\delta^{18}O$-trend considerably, improving paleoenvironmental reconstructions through the main phase of the Great Ordovician Biodiversification Event (GOBE). The new brachiopod carbon and oxygen isotope records from Öland display strong similarity with the East Baltic records, elucidating the regional consistency as well as global correlation utility of the ensuing composite Baltoscandian Lower to Middle Ordovician carbon and oxygen isotope record. The carbon isotope record from Öland indicates that the widely reported Middle Ordovician carbon cycle perturbation—MDICE (Mid-Darriwilian Carbon Isotope Excursion)—is recorded in both brachiopods and bulk carbonates. The oxygen isotope record reveals a long-term Lower to Upper Ordovician trend of increasingly heavier brachiopod $\delta^{18}O$ values, with a pronounced increase during the Middle Ordovician Darriwilian Stage. We interpret this trend as dominantly reflecting a paleotemperature signal indicating progressively cooler Early to Middle Ordovician climate with glacio-eustasy. Our Baltic $\delta^{18}O$ values are therefore consistent with postulations that the biotic radiations during the GOBE and climatic cooling during the Darriwilian were strongly linked.

Plain Language Summary Oxygen isotope values obtained from fossil brachiopod shells have traditionally been used as a faithful paleoclimatic proxy to shed light on temperature trends in ancient oceans. However, because brachiopod shells are susceptible to diagenetic overprint after burial, secular oxygen isotope trends derived from these fossils are often questioned—notably the farther one goes back in geological time. This study presents temporally well-resolved oxygen isotope data from Lower–lower Upper Ordovician sedimentary rocks of Öland, Sweden, tied precisely to conodont biostratigraphy on the bed-by-bed scale. This interval is important in Earth history as it brackets the greatest marine biodiversification event known in the fossil record and coincides with a global climatic cooling phase (determined based on proxies other than oxygen isotopes). The current study therefore provides an excellent test of the spatial and temporal consistency of the secular Ordovician oxygen isotope trend. We find that although our data is probably affected by diagenetic modification, primary paleoclimatic signals are preserved. Furthermore, as current global Ordovician oxygen isotope records lack sufficient resolution because they comprise data from geographically widely distributed low-paleolatitude localities, our new high-resolution data set from one mid-paleolatitude region, provides significant temporal insights that considerably improves our understanding of the Ordovician climate.

1. Introduction

The Ordovician Period was characterized by drastic changes in biodiversity levels and ecosystem engineering (Kröger et al., 2019; C. M. Ø. Rasmussen et al., 2019). Elevated changes in plate movements caused fundamental reorganization of the global paleogeographic configuration as continents rifted off the major continent Gondwana and toward lower latitudes (Cocks & Torsvik, 2005; McKenzie et al., 2014; Torsvik et al., 2012). This

Project Administration: Christian M. Ø. Rasmussen
Resources: Clemens V. Ullmann, Jorge Colmenar, Nicolas Thibault, Gabriella Bagnoli, Svend Stouge
Supervision: Christoph Korte, Christian M. Ø. Rasmussen
Validation: Clemens V. Ullmann, Jorge Colmenar, Nicolas Thibault, Gabriella Bagnoli, Svend Stouge
Visualization: Oluwaseun Edward, Christian M. Ø. Rasmussen
Writing – original draft: Oluwaseun Edward, Svend Stouge, Christian M. Ø. Rasmussen
Writing – review & editing: Oluwaseun Edward, Christian M. Ø. Rasmussen

prominent dispersal of continents may have constituted a first-order control on species richness as provincialism increased (Valentine & Moores, 1970; Zaffos et al., 2017) and contributed to significant changes in global sea level (Hallam, 1992; Haq & Schutter, 2008), which were exacerbated by transient climatic shifts (Barnes, 2004; Finnegan et al., 2011; Fortey & Cocks, 2005; Quinton et al., 2018; C. M. Ø. Rasmussen et al., 2016; Saltzman & Young, 2005; Trotter et al., 2008; Vandenbroucke, Armstrong, Williams, Paris, Zalasiewicz, et al., 2010). Furthermore, carbon isotope excursions hint at major perturbations to the global carbon cycle at this time (Ainsaar et al., 2010; Bergström et al., 2015; Lindskog et al., 2019; Saltzman & Thomas, 2012; Saltzman & Young, 2005), further indicating a coupling between Earth system changes and biodiversity trends during the Ordovician, the most important of which was the Great Ordovician Biodiversification Event (GOBE).

Several hypotheses have been put forward regarding potential triggers of the GOBE including environmental perturbations related to asteroid impact on Earth (Schmitz et al., 2019), changes in weathering patterns and nutrient delivery to the oceans due to the Taconic orogeny (Cárdenas & Harries, 2010; Miller & Mao, 1995), and increased ocean-atmosphere oxygenation (Edwards et al., 2017; Knoll & Carroll, 1999). However, other evidence points to Middle Ordovician climatic cooling and subsequent reduction of physiological stressors on marine organisms as a main driver (Goldberg et al., 2021; C. M. Ø. Rasmussen et al., 2016, 2019; Trotter et al., 2008). The evidence for long-term Ordovician climate change mainly emanates from oxygen isotope compositions of fossil brachiopods and conodonts, which show a secular trend toward generally heavier values from the Early to Late Ordovician. Although different views have been advanced to explain this trend, such as changing seawater oxygen isotope composition, diagenesis, or climate change (Bergmann et al., 2018; Shields et al., 2003; Trotter et al., 2008; Veizer et al., 1999, 2000; Veizer & Prokoph, 2015); sedimentological, sequence stratigraphical and paleontological data have all supported the notion of shorter-term cooling climate, particularly for the Middle Ordovician interval (Dabard et al., 2015; Ghobadi Pour et al., 2007; Le Hérissé et al., 2007; Lindskog & Eriksson, 2017; Nielsen, 2004; C. M. Ø. Rasmussen et al., 2009; J. A. Rasmussen & Stouge, 2018; Turner et al., 2012).

To further test this view during the Lower−Middle Ordovician, the current study presents new high-resolution oxygen and carbon isotope data based on fossil brachiopod and bulk carbonate samples from the island of Öland situated in the Baltic Sea (Figure 1). Particularly in the context of the long-term Ordovician oxygen isotope trend, this interval has been somewhat neglected probably due to the much larger perturbations in the δ^{18}O-record during the earlier and later parts of the Ordovician (Shields et al., 2003; Veizer & Prokoph, 2015; Figure 2). Given that both of these intervals may well have been outside the optimal temperature range for most metazoans as they were either too warm or too cold for latitudinally widespread organismal homeostasis (Clarke, 2014; Pörtner, 2001), even a low amplitude change in temperatures during the Dapingian−Darriwilian global stages could have been significant enough for increasing the carrying capacity of ecosystems as habitable space along the latitudinal gradient increased.

We test the regional consistency of previously reported Baltoscandian Ordovician oxygen isotope trends, as well as the global correlation potential of current global C and O isotope curves (e.g., Shields et al., 2003; Veizer et al., 1999; Veizer & Prokoph, 2015) which remain based on sporadic sampling in the Ordovician interval. Thus, the current study enables, for the first time, an intra-basinal comparison of fossil brachiopod carbon and oxygen isotope compositions spanning the Lower Ordovician (Floian) to Middle Ordovician (Darriwilian) interval. Additionally, material is also sampled through to the Upper Ordovician (upper Sandbian), complementing the global Ordovician stable isotope record by adding better temporal resolution tied precisely to conodont biostratigraphy.

2. Geological Setting

The paleocontinent of Baltica comprises most of northern Europe and consists of Archean and Proterozoic rocks forming the East European craton (Cocks & Torsvik, 2005). The Ural Mountains in the East, the Trans-European Suture Zone to the south-west, and the Scandinavian Caledonides in the north-west border this paleocontinent. During the earliest Cambrian, Baltica rifted off the continent of Gondwana, which opened the Tornquist Sea to the southwest and separated Gondwana and Baltica. The drifting phase of Baltica was associated with counterclockwise rotation starting in the mid-Cambrian and lasted into the Middle Ordovician (Torsvik & Rehnström, 2003). Baltica moved from high southerly to intermediate latitudes by the Middle Ordovician and continued toward the paleoequator throughout the Ordovician (Cocks & Torsvik, 2005; Torsvik et al., 1992, 2012). In this period, the passive margin was influenced by continental thermal subsidence and first and second-order

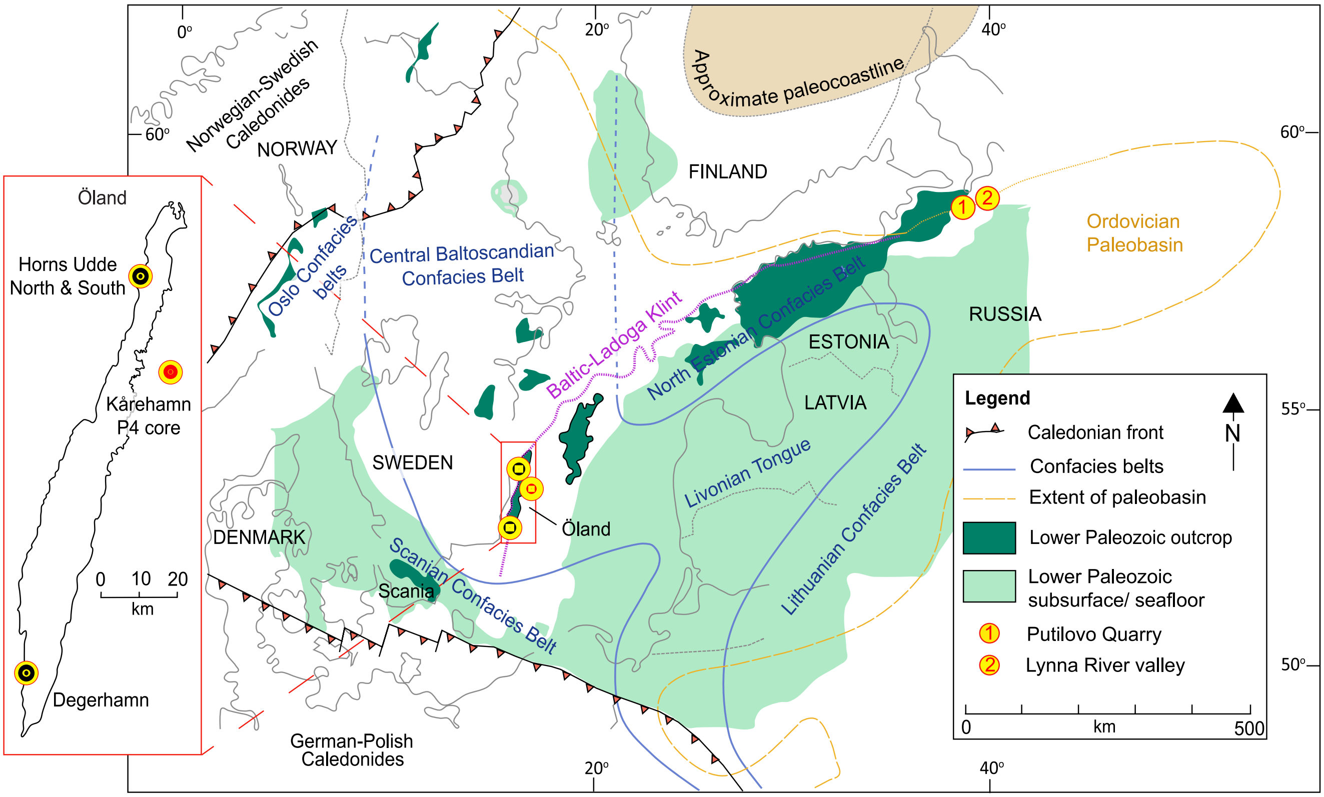

Figure 1. The confacies belts of the Ordovician Baltoscandian Paleobasin with the lower Paleozoic outcrop and subsurface extent shown. Localities discussed in the text are highlighted. Insert map of Öland shows an enlarged view of the current study's sampling sites. Modified after Jaanusson (1982a).

sea-level rises, which resulted in the generation of an extensive epicontinental sea with an unusual low-relief topography (Nielsen, 2004; Torsvik & Cocks, 2016).

The Baltic paleocontinent remained tectonically calm until the Middle Ordovician and was bounded by the Tornquist Sea to the southwest and the Iapetus Ocean to the northwest. As the microcontinent Avalonia reached Baltica, volcanism commenced, which became evident in the Sandbian (early Late Ordovician) during which a complex of bentonites appeared on Baltica as subduction beneath Avalonia began (Huff et al., 1992; Torsvik & Rehnström, 2003). This phase likely started already during the lower Darriwilian as numerous bentonites are found in southernmost Swedish (Scanian) shale deposits as well as in contemporaneous carbonate successions in Sweden (Bagnoli & Stouge, 1999; Lindskog et al., 2017).

The Ordovician Baltoscandian Paleobasin is a major feature of Baltica (Figure 1). It trends west-southwest (WSW) to east-northeast (ENE) and paleocurrents responsible for the transportation of sediment within the basin were in SW to NE directions (Kiipli et al., 2009). The deposition of the Lower to Middle Ordovician sedimentary successions in the basin took place in epicontinental seawater conditions on the shelf of a stable craton (Jaanusson, 1995; Männil, 1966). In this calm period, the sedimentary deposits were extensive and covered the areas of Scandinavia, the East Baltic countries, and eastern Russia, Ukraine, and northern Poland culminating during the sea-level highstand in the Floian (*evae* transgression; Early Ordovician; Nielsen, 2004). Sediment accumulation was slow and middle Cambrian to Middle Ordovician deposits were condensed, which resulted in the fine clastic and organic-rich Alum Shale Formation that persisted from the Cambrian into the Lower Ordovician and the overlying carbonate blanket of the Lower to Middle Ordovician Orthoceratite Limestone (Stouge, 2004).

The characteristic lithofacies arrangement of Männil (1966) was combined with the faunal distribution and divided into broad confacies belts (Jaanusson, 1976, 1982a, 1995; Figure 1). These belts differ from each other in types of sedimentation, faunal diversity, and abundance. Öland experienced little burial, although there is a gradient from thermally immature rocks in the North (CAI: 1) to early mature rocks (CAI: ca. 1.5) in the South (Bergström, 1980; Tullborg et al., 1995).

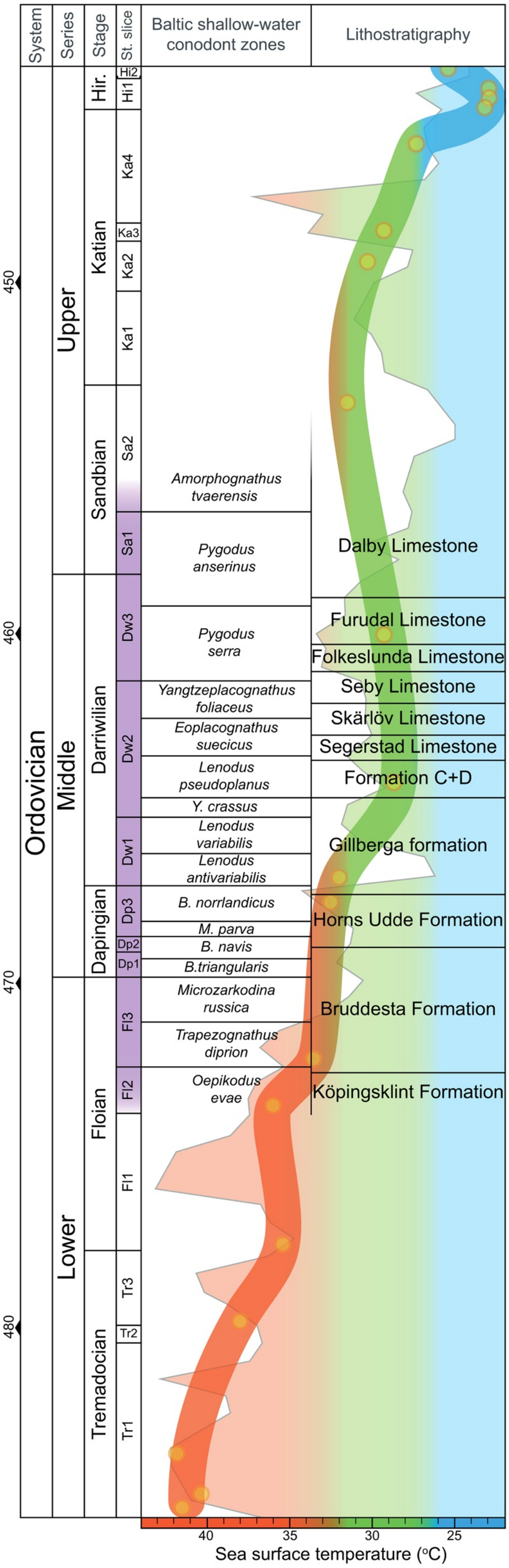

Figure 2.

Due to widespread Ordovician outcrops and well-preserved fossils, a relatively simple tectonic regime with the absence of significant thermal alteration, the Baltoscandian Paleobasin in general, and Öland, represents an ideal site for investigating the Lower−Middle Ordovician carbon and oxygen isotope record.

3. Lithostratigraphy and Biostratigraphy

The Lower to Middle Ordovician (Floian to middle Darriwilian) Orthoceratite Limestone on Öland is composed of green, gray, and red carbonate sedimentary rocks. The limestone is highly condensed, often glauconitic, and with low-diversity skeletal composition (Figure 3). Many diastems occur in the succession and these are commonly marked by discontinuity surfaces (Jaanusson, 1961; Lindström, 1979) and less commonly, burrowed, and mineralized corrosion hard ground/firm grounds are present (Ekdale & Bromley, 2001). The average carbonate accumulation rate and low siliciclastic input were in the order of 1–4 mm per 1,000 years and sea-level fluctuation was a significant factor for the lithofacies development (Chen & Lindström, 1991; Jaanusson, 1982b; Lindskog et al., 2017; Lindström, 1984; Stouge, 2004). According to the confacies belts of Jaanusson (1976, 1995), the island of Öland lies within the Central Baltoscandia confacies belt, where the northern part is closer to the Estonian confacies belt than the southern part of the island (Figure 1).

The Öland coastal cliff sections, onshore drill cores, and the Kårehamn offshore drill core (Bohlin, 1949, 1953; Stouge, 2004; Wu et al., 2017) are assigned to 12 lithostratigraphic units, although some of them are informal. The entire upper Lower to lower Upper Ordovician succession is further biostratigraphically well constrained based on conodonts. The litho-, bio-, and chronostratigraphic schemes used here as reference are shown in Figure 2 and have been compiled based on information from several sources (Bagnoli & Stouge, 1997; Bergström, 1971, 2007; Bergström et al., 2009; Lindström, 1971; Löfgren, 2000, 2003; Stouge, 2004; Stouge & Bagnoli, 1990; Stouge et al., 2020; van Wamel, 1974; Wu et al., 2017; Zhang, 1998).

3.1. Deposition of the Orthoceratite Limestone

The Lower to Middle Ordovician succession on Öland is composed of carbonates, mud-rich carbonates, and marly limestones deposited below normal but above storm wave base (Dronov & Rozhnov, 2007; Dronov et al., 2011). The succession is commonly bioturbated and sedimentary structures are rarely preserved, suggesting that abundant benthic life prevailed on the sea floor. The strata are well-bedded and are characterized by the presence of hardgrounds, as well as burrows which are parallel to bedding (*Planolites*; Ekdale & Bromley, 2001; Ekdale et al., 2002; Jaanusson, 1961; Lindström, 1963, 1979). These horizontal burrows are commonly filled with micritic mud and cement. In addition, stylolite formation is commonly observed. Also, characteristic for the investigated succession at Horns Udde, is the interval composed of red carbonate beds (red-brown limestone of the Brudddesta and Horns Udde formations) that overlie the gray-green glauconite-bearing carbonates of the Köpingsklint Formation. These strata are overlain by the rhythmic deposition of glauconite-rich, coarse-grained limestone, and silty limestone, which are assigned to the Gillberga Formation (Stouge, 2004). The most common allochems include bryozoans, cephalopods, echinoderms, and trilobites (Bohlin, 1949; Eriksson et al., 2012; Lindström, 1984; van Wamel, 1974). Based on the content and presence of these allochems a succession composed of trilobite-bearing wackestone/pack-

10.1029/2021PA004309

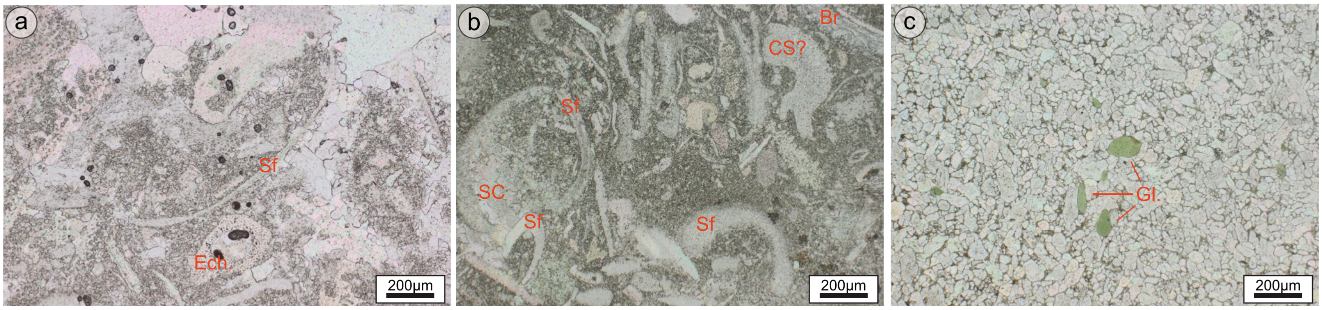

Figure 3. Photomicrographs showing carbonate microfacies in the study area. Sf = undifferentiated skeletal fragments, Ech. = echinoderm, SC = sparry calcite, CS? = cephalopod shell, Br = brachiopod shell, Gl. = glauconite grain. (a)**,** Sample OLK-16, bioclastic packstone, Sandbian. (b), Sample OLD-1, bioclastic packstone, Darriwilian. (c), Sample OLH-11, glauconitic grainstone, Floian. Scale bar is 200 µm.

stone, echinoderm wackestone/packstone, and trilobite glauconite-bearing wacke-to packstone with variable mud content can be distinguished throughout the succession. The lowermost and topmost formations of the succession, that is, the Köpingsklint and Gillberga formations, represent an offshore proximal margin, whereas the middle part contains the Bruddesta and Horns Udde formations, were deposited in a more offshore distal setting.

The red mud-rich limestone exposed at the Horns Udde section was deposited in tranquil and fair-weather conditions and accumulated by mud suspension in a relatively deeper-water setting. These red strata were probably a result of the ventilation and oxygenation of Fe-rich sediments on the sea bottom. The temporal and spatial distribution of these red-brown limestones is associated with regional sea-level changes and their formation was presumably induced by global transgression in association with the drowning of the Baltic platform (i.e., the *evae* transgression; Nielsen, 2004; Stouge et al., 2020). The upper glauconite-rich and high-energy carbonates with transported shells and fossil debris were deposited during high-energy or storm events forming tempestites (Bohlin, 1949; Dronov & Rozhnov, 2007).

3.2. Sampled Successions

3.2.1. Horns Udde North Section

The Horns Udde North section lies ca. 1.5 km to the northeast of the Cape of Horns Udde (Figure 1). The complete sedimentary succession comprises Cambrian to lower Middle Ordovician (Darriwilian) sedimentary rocks. However, the Cambrian and the lowermost Ordovician (lower Tremadocian) strata in the beach zone are completely covered by rubble. The section has been described in detail by Lindström (1963), Tjernvik (1956), and van Wamel (1974), and the most recent conodont zonation has been provided by Bagnoli and Stouge (1997) who sampled the section thoroughly in high resolution (Figure 4). The exposed succession consists of glauconitic siltstone, nodular gray to red mottled limestone, and gray to reddish-brown green mottled limestone with marly interbeds and several discontinuity surfaces. The Horns Udde section represents the mud-rich portion of the middle-ramp and proximal portion of the outer ramp environment characterized by an abundance of glauconite.

The succession is referred to the Köpingsklint, Bruddesta, Horns Udde, and Gillberga formations respectively, with the Lower−Middle Ordovician boundary placed within the Bruddesta Formation (Stouge, 2004; van Wamel, 1974; Figure 4). Dome-like structures and a pronounced hardground complex known as "Blommiga bladet" (= "Flowery sheet" in English); see Figure 4 (Bohlin, 1949; Ekdale & Bromley, 2001) lies within the Bruddesta Formation. Just above the base of the Horns Udde Formation, three distinct horizons, collectively 0.2 m thick, and composed of prominent hematite-impregnated bacterial-like structures occur (named "Blodläget" = "Bloody layer" in English (Bohlin, 1949; Stouge, 2004)). The uppermost 2.3 m of strata in the section belong to the lower sub-unit of the overlying Gillberga Formation (= Formation A of Stouge (2004)). These beds are composed of unevenly bedded, glauconitic limestone with some intervals of nodular limestone interbedded with minor green glauconite shale.

Figure 2. Ordovician chronostratigraphy and paleothermometry. The studied interval is highlighted in purple with the litho- and conodont biostratigraphy of northern Öland shown. Numbers on far left are in million years. The paleothermometry is based on ^{18}O-conodont apatite (Trotter et al., 2008) and ^{18}O-bulk rock (Goldberg et al., 2021). Orange colors denote temperatures above present-day tropical sea surface average, green shading present-day window, and blue shading below present-day levels. Note that the present-day temperature window is reached during the Dapingian−lowermost Darriwilian.

10.1029/2021PA004309

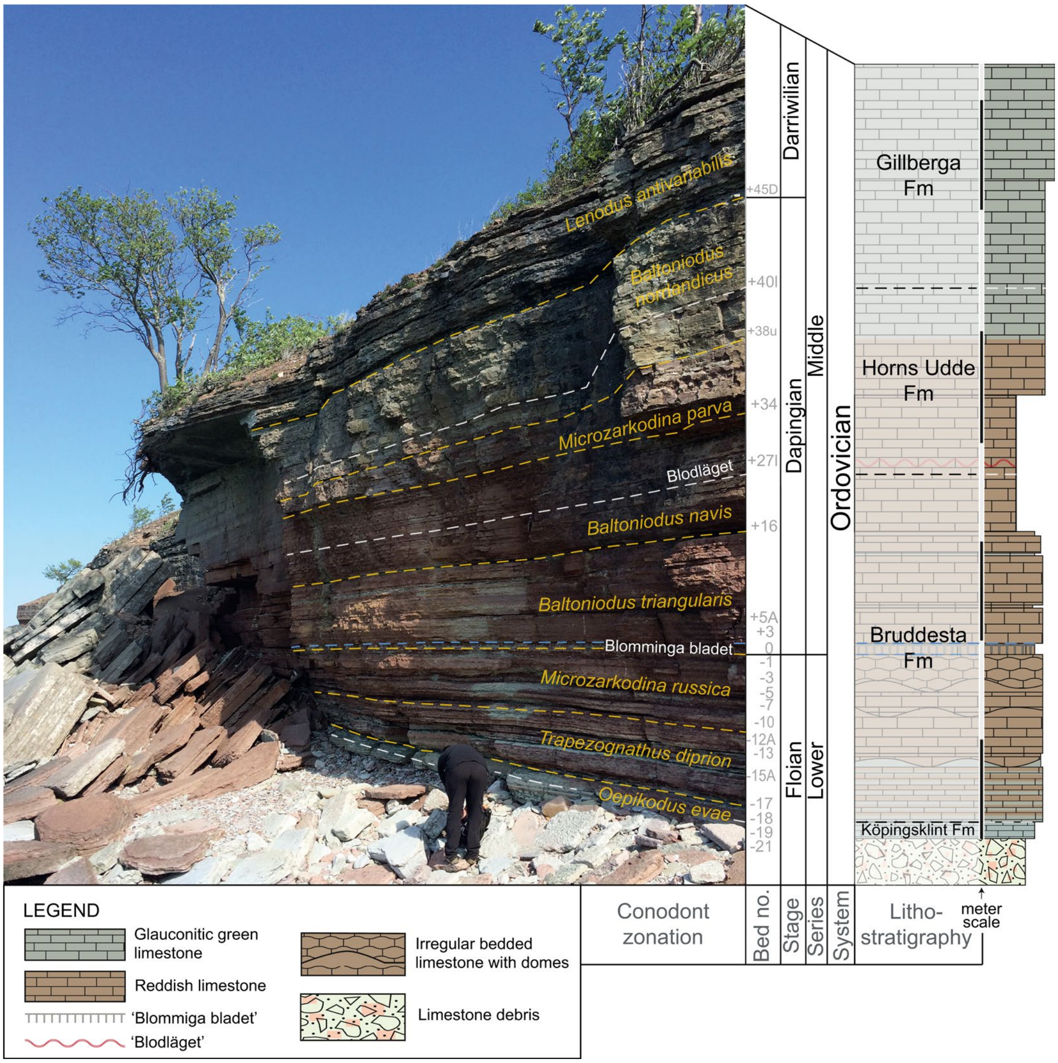

Figure 4. Field photo of the locality at Horns Udde North, northern Öland. Lithological units and boundaries are shown in white. Conodont biostratigraphical zonal boundaries based on Bagnoli and Stouge (1997) are shown in orange and tied to global stratigraphy (right). The bed numbering system applied in the current study is also shown. The idealized log (right) shows main lithological features, unit names, and thickness of profile. See legend for details.

The Lower to Middle Ordovician succession at the Horns Udde North section (Figure 4) was sub-divided into eight conodont zones by Bagnoli and Stouge (1997) and van Wamel (1974) and partitioned into 101 beds, including sub-beds, from which brachiopods were collected. This has allowed for detailed bed-by-bed correlation tied accurately to the conodont biostratigraphy through the roughly 8-m-thick section.

3.2.2. Horns Udde South Section

This locality is located at the Cape of Horns Udde (Figure 1). The succession covers the top of the Horns Udde Formation and reaches approximately two meters higher into the overlying Gillberga Formation than the section North of Horns Udde. The succession starts with the reddish-colored Horns Udde Formation, of which the *B. navis*, *Melanotaenia parva,* and *B. norrlandicus* conodont zones are found (Figure 5). About midway through the latter conodont zone lies the formational boundary between the Horns Udde and the Gillberga formations.

The Gillberga Formation is lithologically similar to the Horns Udde North section (see above), being greyish-green and unevenly bedded. It is about 4.1-m thick at this locality, thus potentially yielding up to 2 m of new section compared to the section North of Horns Udde. Toward the top of this section, abundant glauconite grains

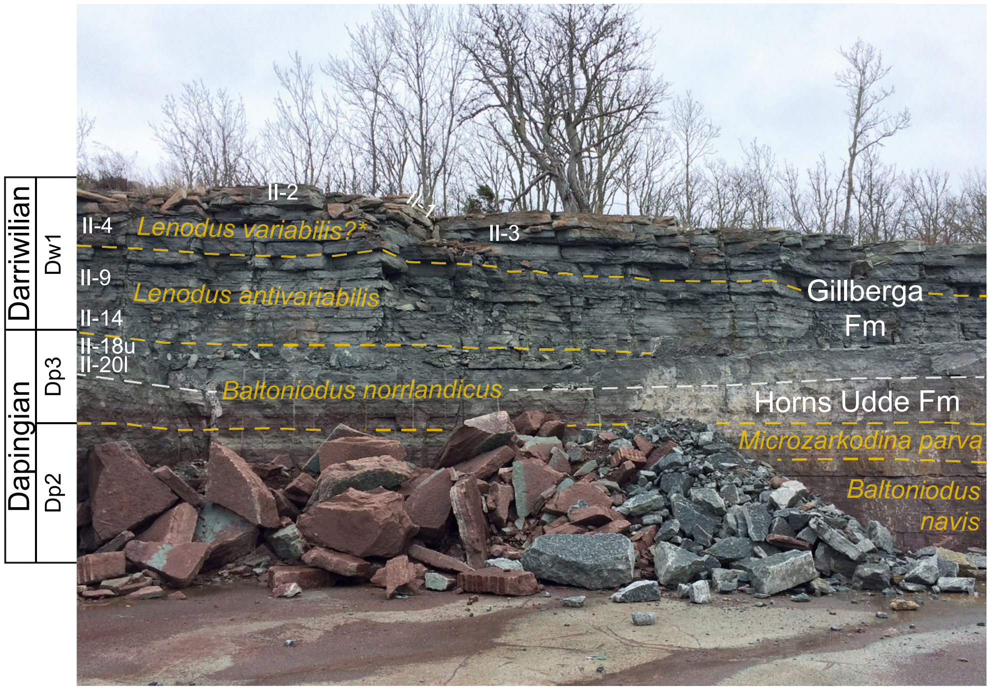

Figure 5. Field photo of the auxiliary section, Horns Udde South, northern Öland. Lithological units and boundaries shown in white and conodont biozones of Bagnoli and Stouge (1997) in orange. Bed numbering system is also indicated at unit boundaries. The section is ca. 5.5 m thick of which the upper 4.1 m were sampled.

characterize the rocks. Although the upper beds did not yield diagnostic conodont elements to aid biostratigraphic assignment, the associated brachiopod fauna is very characteristic of the lowermost Kunda Regional Stage. We are therefore confident that these beds are coeval with the *Lenodus variabilis* Conodont Zone. In this section, the Gillberga Formation was sampled from its base and divided into 32 beds, all of which yielded brachiopods.

3.2.3. Kårehamn P4 Drill Core

The sampled Kårehamn P4 core was drilled ca. 5 km offshore and to the east of the Kårehamn harbor (Figure 1). The borehole penetrated about 40 m of Ordovician limestone covering Middle and lower Upper Ordovician strata (middle Darriwilian to upper Sandbian) and the succession is typical for the Baltoscandian Paleobasin (Figure 6). The detailed description and conodont biostratigraphical analysis of the core is not published and work on the succession is still in progress.

The base of the drillcore (at −64.5 m below the sea floor) is characterized by the upper part of the glauconite-bearing Gillberga Formation (Figure 6) and is, thus, stratigraphically very close to the interval covered by the section at Horns Udde South. It is within the upper *L. variabilis* Conodont Zone and is immediately followed by the *Yangtzeplacognathus crassus* Conodont Zone (Dw2, Middle Ordovician). The strata from −62.9 to −54.9 m (Formations C and D) are referred to the *Lenodus pseudoplanus* Conodont Zone (with the *Microzarkodina hagetiana* and *M. ozarkodella* subzones, Dw2). The overlying Segerstad and Skärlöv limestones (−54.8 to −50.2 m) are referred to the *Eoplacognathus suecicus* Conodont Zone *s.l.* The *Yangtzeplacognathus foliaceus* Conodont Zone (−51.1 to −49.6 m) is recorded from, and characterizes, the strata that are assigned to the Seby Limestone. There is a minor hiatus near the base of the *P. serra* Zone that is marked by a prominent discontinuity surface (D at −50.1 m on Figure 6). The *Eoplacognathus reclinatus* and *E. robustus* subzones of the *Pygodus serra* Conodont Zone are recorded from the Folkeslunda and Furudal limestones.

The lower 19.1 m of the core is assigned to the Orthoceratite Limestone, which concludes with the Folkeslunda Limestone at −47 m (Figures 3 and 6). The *Pygodus serra* Conodont Zone starting from the Folkeslunda Limestone represents the base of the uppermost third of the Darriwilian Stage (Dw3, upper Middle Ordovician). The

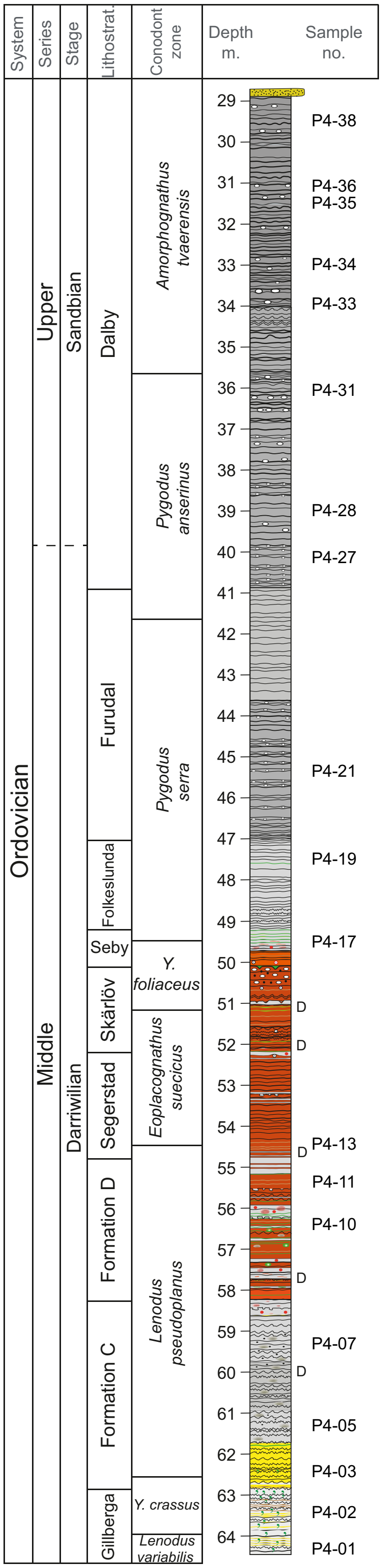

Figure 6.

Pygodus anserinus Conodont Zone is recorded from −41.7 m near the base of the Dalby Limestone and is succeeded by the *Baltoniodus variabilis* Subzone of the *Amorphognathus tvaerensis* Conodont Zone.

The top of the core (−29 m) is within the lower upper Sandbian (Upper Ordovician) Dalby Limestone (Figure 6). The *Amorphognathus tvaerensis* Zone and the *Baltoniodus variabilis* Subzone encompass this unit and extend to the top of the core. The base of the Upper Ordovician Series (Sandbian Stage) is tentatively placed ca. at –39.8 m in the core (Figure 6). The core was sampled for brachiopods at 1-m resolution and 19 beds yielded samples that could be analyzed (Figure 6).

3.2.4. Degerhamn Quarry

The Degerhamn Quarry (Figures 1 and 7) is an active limestone quarry, which is accessible by permission of the company that operates the quarry. The complete succession in the quarry extends down to the Cambrian Alum Shale Formation (Stouge, 2004), however, today this is covered by water. The exposed portion in the active quarry comprises the Gillberga Formation, which is composed of bedded, gray limestone superposed by various colors extending from green, red to violet. The overlying gray to green marker, locally known as "Sphaeronites" bed, ca. 0.9-m thick, is composed of grainstone to packstone containing accumulations of "*Echinosphaeronites*" in the middle of the unit (Stouge, 2004; see Figure 7). The coeval bed in south-central Sweden is referred to as the Täljsten (Eriksson et al., 2012). The upper part of the quarry consists of gray to mottled red or red-brown limestone.

The exposed succession in the active quarry is of Darriwilian Age (Stouge, 2004; Stouge & Bagnoli, 2014). The lower part, composed of gray multi-colored limestone, is referred to the *Lenodus antivariabilis* and *L. variabilis* zones. The green-gray "Sphaeronites" bed is referred to the *L. variabilis* zone up to the accumulation of "*Echinosphaeronites*," which is in the *Y. crassus* Conodont Zone. The upper part of the succession exposed in the quarry is assigned to the *Microzarkodina hagetiana* subzone of the *Lenodus pseudoplanus* Zone. From this locality, nine samples were collected through the *L. antivariabilis* to *L. variabilis* interval, and they are thus all placed within the Middle Ordovician Darriwilian Stage (Dw1).

Importantly, this locality provides samples from more deeply buried rocks ca. 100 km South of the other three studied localities, thus, enabling the assessment of potential diagenetic impact by burial depth on carbon and oxygen isotope compositions within the *L. antivariabilis* Conodont Zone across Öland.

4. Materials and Methods

Fossil brachiopods (n = 185) and whole rock samples (micrite, n = 156) were collected from the localities described above (Figures 1 and 4–7). Samples from the Horns Udde North and South sections were collected bed-by-bed. The distance between the samples from the Degerhamn Quarry section, South Öland, varies, but is about 40 cm. Fossil brachiopods, as well as the bulk carbonate (micrite) in which they were embedded, were collected at approximately one-m intervals from the Kärehamn P4 core (Figure 1). All analyzed materials are stored at the Natural History Museum of Denmark.

10.1029/2021PA004309

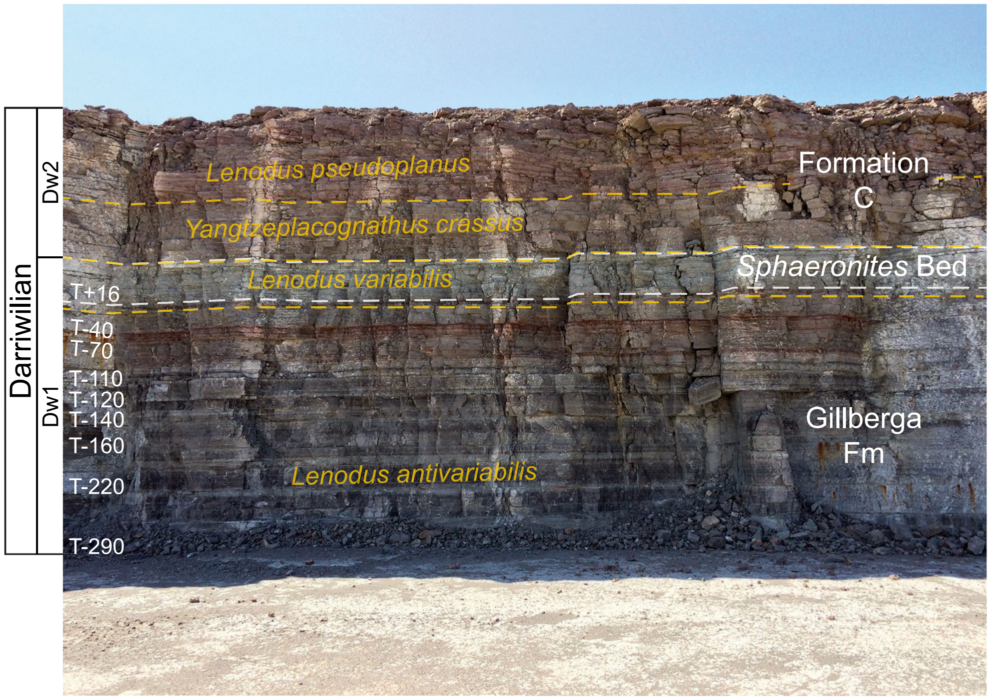

Figure 7. Field photo showing the studied outcrop in the Degerhamn Quarry, South Öland. Lithological units and informal names are written in white with corresponding white punctuated lines. Conodont biozonation, based on Stouge (2004) and Stouge and Bagnoli (2014), is highlighted in orange with corresponding punctuated lines. The stratigraphical position of the samples obtained from this section is shown in white to the left. The section is ca. 5 m thick.

4.1. Sampling Routines

Some brachiopods were sampled multiple times, hence, the total number of processed samples for geochemical and isotopic analysis is 226 brachiopod and 169 bulk rock samples. Brachiopods were cleaned using a brush and inspected for preservation under a binocular microscope. Splinters from the secondary shell layer of brachiopods were collected using a stainless-steel needle. Whole rock powder was extracted from the matrix adjacent to the sampled brachiopod shells using a handheld drill with a diamond-coated steel bit of ca. 1 mm diameter under a microscope. Rock surfaces were mechanically abraded, and micrite was extracted from the rock matrix, avoiding weathered parts and calcite veins.

4.2. Scanning Electron Microscopy

Shell splinters from the secondary shell layer of brachiopods were checked for textural preservation using scanning electron microscopy (SEM; Figure 8). Shell splinters were mounted on an adhesive stub and subsequently gold coated before screening. SEM analysis was conducted at the Natural History Museum of Denmark using an FEI Quanta 250 SEM in high vacuum mode.

4.3. Carbon and Oxygen Isotopes

Carbon and Oxygen isotope measurements of brachiopod shell material and whole rock powder were generated using an IsoPrime triple collector Gas Source Isotope Ratio Mass Spectrometer with a Multiflow unit at the University of Copenhagen following the procedures outlined by Ullmann et al. (2013). In summary, about 0.8 mg

Figure 6. Lithology and sample levels of the Kårehamn P4 core tied to bio-and lithostratigraphy. The lithostratigraphical names are mainly informal with some of the units either being topo-formations (e.g., Jaanusson, 1960), traditional units (e.g., Bohlin, 1949, 1953), or informal units (Stouge, 2004). Conodont biozonation established by GB and SS based on core material and follows the biostratigraphy developed by Stouge and Bagnoli (1990), Bagnoli and Stouge (1999). Note the sampling levels for the current study on the far right.

10.1029/2021PA004309

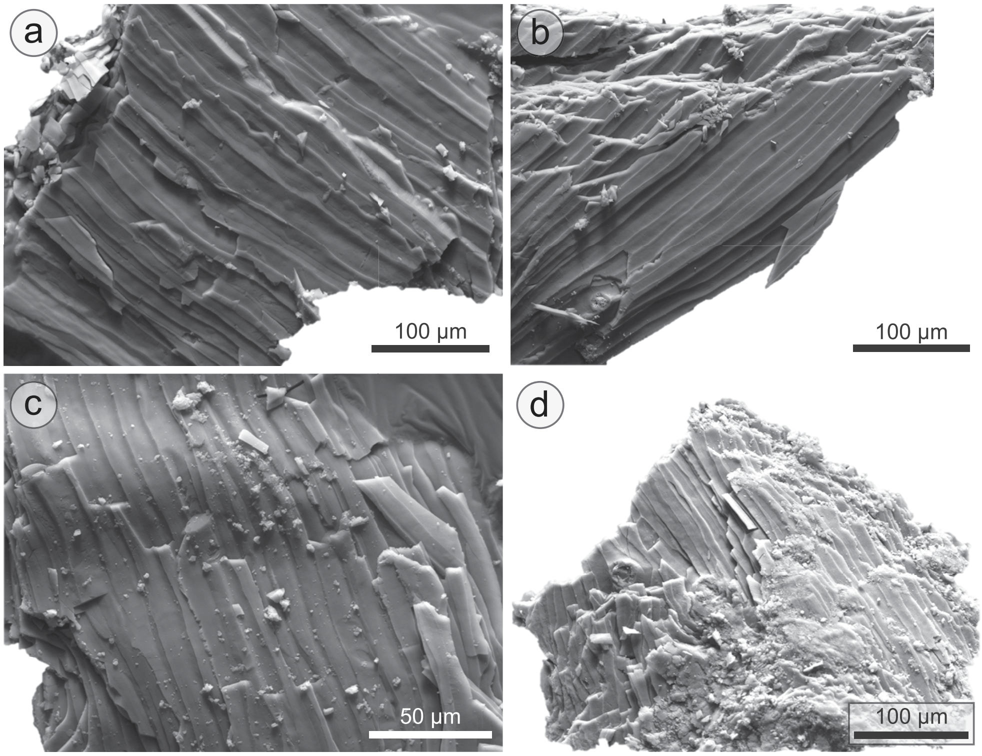

Figure 8. SEM images of Ordovician brachiopod shell material. (a) Sample OLH-19, mid Floian, Köpingsklint Formation, Horns Udde North. (b) OLH-64, mid-Dapingian, Horns Udde Formation, Horns Udde North. (c) Sample OLK-3, upper Darriwilian, Folkeslunda limestone, Kärehamn P4 core. (d) OLH-98, lower Darriwilian, Gillberga Formation, Horns Udde North. Specimens (a–c) show texturally well-preserved secondary shell layers and specimen (d) is characterized by partial recrystallization.

of sample material placed in glass vials were dissolved with ca. 0.05 ml of >100% concentrated phosphoric acid (H_3PO_4) and left to react for 90 min at 70°C. $\delta^{13}C$ and $\delta^{18}O$ compositions were measured from the resulting carbon dioxide. Data were corrected for weight-dependent biases by using the University of Copenhagen in-house reference standard—LEO (finely crushed Carrara marble). Reproducibility of the measurements, as determined from the standard deviation of LEO is better than 0.1‰ for $\delta^{13}C$ and $\delta^{18}O$.

4.4. Element/Ca Ratios

Element/Ca ratios (Sr/Ca and Mn/Ca) were measured from the reacted carbonate remains of brachiopod subsamples using an Agilent 5110 VDV Inductively Coupled Plasma Optical Emission Spectrometer (ICP-OES) at the University of Exeter, Penryn Campus following the procedure outlined in Ullmann et al. (2020). Accuracy of the analysis was controlled through multiple analyses of a synthetic quality control solution—BCQC ($n = 4$) and the international reference materials—AK ($n = 8$) and JLs-1 ($n = 12$). Analytical bias, determined via the deviation of measured element/Ca ratio from the expected value in the gravimetrically prepared quality control solution—BCQC, was ≤0.5% for each of the reported element/Ca ratios.

5. Results

All carbon and oxygen isotope compositions of brachiopods and bulk rocks and their relations to their element/Ca ratios are summarized in Figure 9 and all data are presented in Figure S2, as well as the Supporting Information datafile. In Figure 9, the new data are plotted together with literature data from well-preserved coeval samples from the eastern part of the Baltoscandian Paleobasin (St. Petersburg region, C. M. Ø. Rasmussen et al., 2016).

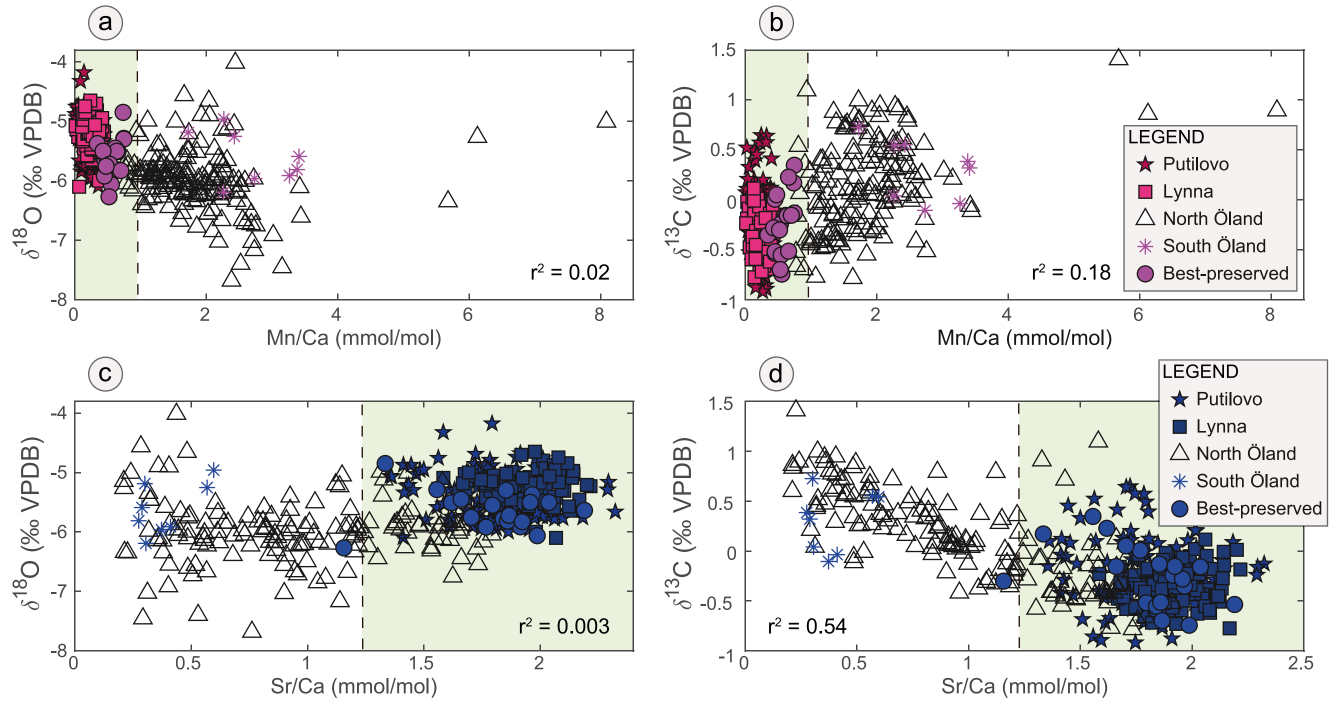

Figure 9. Scatter plots showing correlation between element/Ca ratios and $\delta^{18}O$ and $\delta^{13}C$ values of investigated brachiopods in the current study and the East Baltic data set (Putilovo and Lynna, C. M. Ø. Rasmussen et al., 2016). (a) Scatter plot of Mn/Ca versus $\delta^{18}O$. (b) Scatter plot of Mn/Ca versus $\delta^{13}C$. (c) Scatter plot of Sr/Ca versus $\delta^{18}O$. (d) Scatter plot of Sr/Ca versus $\delta^{13}C$. Element/Ca data interpreted as best-preserved if Mn/Ca $\leq$ 1 mmol/mol. In most cases these samples also have Sr/Ca ratios $\geq$1.3 mmol/mol. Vertical dashed lines with green shading represent preservation limits. Samples labeled as best-preserved are a subset of the entire Öland data set and are not unique to any of the localities sampled on Öland (see also Figures 10 and S1). Values of r^2 only refer to the Öland data set.

5.1. Carbon Isotopes

Carbon isotope values of brachiopods ($\delta^{13}C_{brachiopod}$) vary between −0.8‰ and +1.4‰ and whole rock carbonates ($\delta^{13}C_{bulk}$) between −1.0‰ and +1.6‰. Both data sets follow the same general temporal trend (Figure 10). $\delta^{13}C_{brachiopod}$ values are generally lighter than $\delta^{13}C_{bulk}$, being offset by approximately 0.5‰. Both $\delta^{13}C_{brachiopod}$ and $\delta^{13}C_{bulk}$ are characterized by an increasing trend during the Floian, showing a range of −0.3‰ to +1.0‰. This is followed by a decline of about 1.7‰ in $\delta^{13}C_{brachiopod}$ from the Floian–Dapingian transition to the end of the Dapingian (*B. triangularis* to the top of the *B. norrlandicus* conodont zones). For $\delta^{13}C_{bulk}$, the decrease is less severe as $\delta^{13}C$ values only plunge by ca. 0.8‰ before stabilizing in the lower Darriwilian *L. antivariabilis* Conodont Zone to +0.3‰. Beginning in the *Y. crassus* Conodont Zone, a positive excursion takes place in both $\delta^{13}C_{brachiopod}$ and $\delta^{13}C_{bulk}$ which culminates in the middle Darriwilian *E. suecicus* Conodont Zone. Here, peak values of +1.4‰ and +1.6‰ are recorded for $\delta^{13}C_{brachiopod}$ and $\delta^{13}C_{bulk}$ respectively. Subsequently, in the upper Darriwilian and Sandbian, $\delta^{13}C_{brachiopod}$ and $\delta^{13}C_{bulk}$ values decrease by ca. 0.6‰ but remain heavier than during pre-excursion times, ranging between +0.2‰ and +1.0‰.

5.2. Oxygen Isotopes

The oxygen isotope record exhibits a general long-term Ordovician increasing trend and most notably, a sustained rise during the Darriwilian (Figure 10). Brachiopod $\delta^{18}O$ values are typically offset by +0.6‰ relative to $\delta^{18}O_{bulk}$ (see Figure S2) and vary by up to 1‰ within individual brachiopod beds. Bulk rock $\delta^{18}O$ composition ranges from −8.0‰ to −4.9‰ in the studied interval and between −7.7‰ and −4.0‰ for brachiopods. The Floian is characterized by an increase of up to 1.8‰ in both brachiopods and bulk rocks, before reverting to background values of about −6‰ at the Floian–Dapingian transition (*B. triangularis* Conodont Zone). The Dapingian data set is characterized by an initial increase of ca. 1.5‰ in both $\delta^{18}O_{bulk}$ and $\delta^{18}O_{brachiopod}$, followed by a decrease of up to 2‰ reaching into the lower Darriwilian. Within the lower Darriwilian (*L. antivariabilis* Conodont Zone), both brachiopods and bulk rocks display a wide $\delta^{18}O$ range of 1.9 and 3.0‰, respectively. Notably, the lowest

10.1029/2021PA004309

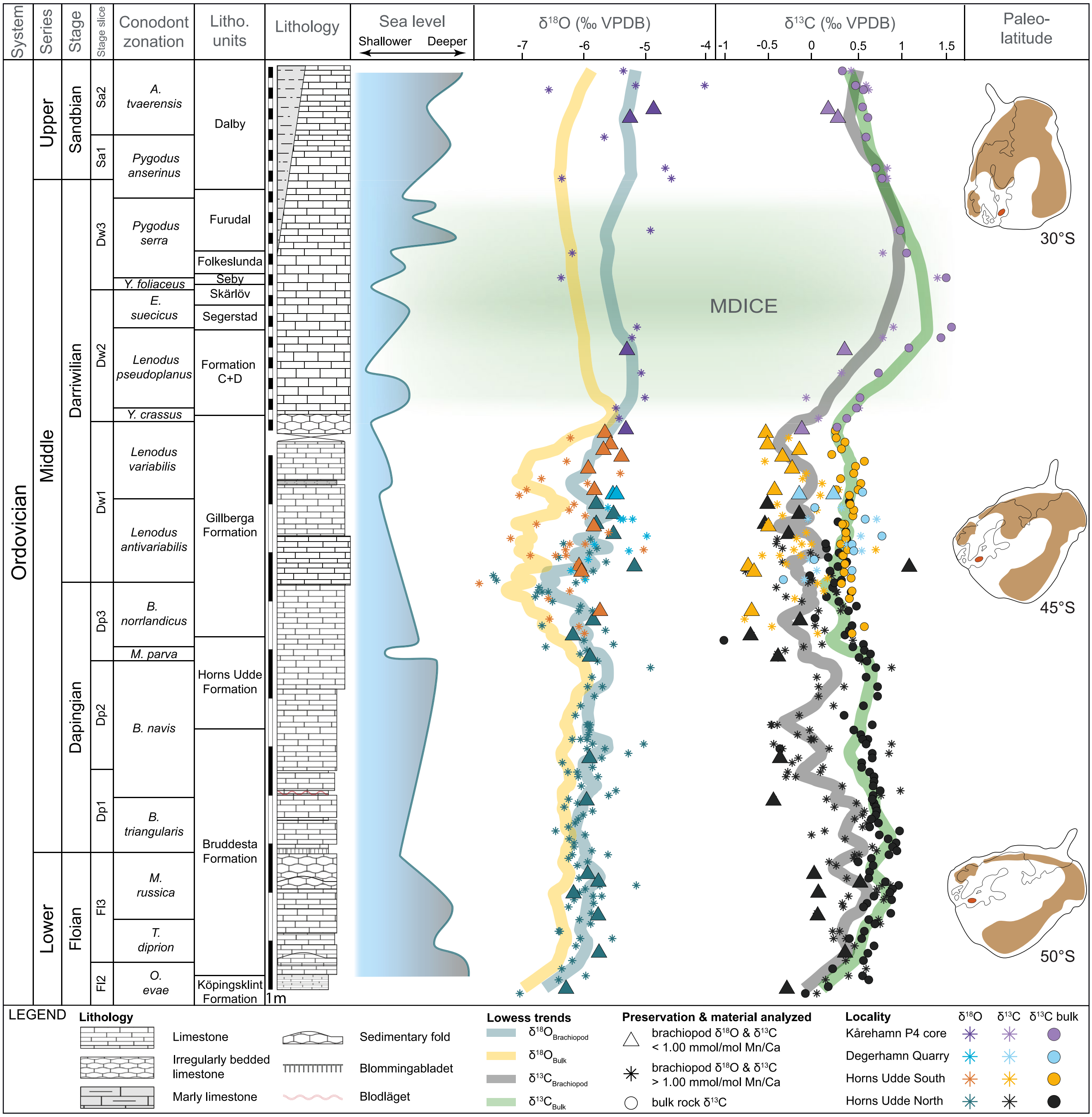

Figure 10. Summary figure showing carbon and oxygen isotope compositions of investigated fossil brachiopods and bulk carbonates through the studied composite interval as well as our interpreted relative sea-level curve up through the succession (based on lithology and conodont biofacies (see Bagnoli & Stouge, 1996). The four different localities studied are represented by their own shading. A 10-point LOWESS smoothing has been applied to accentuate temporal trends in the data set using the software OriginPro. Yellow LOWESS curve represents bulk oxygen values plotted in the Supplementary Information Figure 2 (but omitted from this figure to reduce data point cluttering). A pronounced positive $\delta^{13}C$ excursion is apparent in both bulk carbonates and fossil brachiopods during the Middle Darriwilian (MDICE), as well as a sustained Darriwilian increase in $\delta^{18}O$. Note that samples below the operational limit of preservation all fall within the range of the samples above the cutoff limit. The data set is not evenly scaled as the middle Darriwilian to Sandbian part of the figure is vertically compressed due to reduced sampling resolution in this interval.

10.1029/2021PA004309

$\delta^{18}O$ values in this interval correspond to samples from North Öland, whereas those from Degerhamn, South Öland, are characterized by the heaviest $\delta^{18}O$ values. Beginning in the *L. variabilis* Conodont Zone, brachiopod $\delta^{18}O$ values steadily increase by up to 1.5‰ into the lower *E. suecicus* Conodont Zone. This is followed by a decrease of ca. 1‰ until the base of the *P. serra* Conodont zone (upper Darriwilian). Subsequently in the upper Darriwilian to Sandbian (*P. serra* to *A. tvaerensis* Conodont Zone) interval, $\delta^{18}O$ values of bulk carbonates and brachiopods show no clear pattern, but instead vary significantly by up to 2.5‰.

5.3. Element/Ca Ratios

Element/Ca ratios of investigated brachiopods vary between 0.21 and 2.19 mmol/mol for Sr/Ca and 0.34 and 8.09 mmol/mol for Mn/Ca. Element/Ca ratios do not vary distinctly between localities, and do not display discernible stratigraphic trends (Figure S1). Correlation between element/Ca ratios and isotopic compositions is observed in the case of Sr/Ca and $\delta^{13}C$ (Figure S3), with negative slope of $\Delta^{13}C$ (the difference of brachiopod and bulk carbonate $\delta^{13}C$) versus Sr/Ca and $\delta^{13}C$ versus Sr/Ca suggesting a link between depletion in Sr/Ca and $\delta^{13}C$. These element/Ca trends diverge from those documented for the Eastern Baltic (Figure 5; C. M. Ø. Rasmussen et al., 2016), hinting at variability in trace element patterns in sediments within the Baltoscandian Paleobasin.

6. Discussion

6.1. Screening of Samples

A combination of optical (Scanning Electron Microscopy), chemical (element/Ca ratios) and statistical methods (correlation between element/Ca ratios and $\delta^{13}C$, $\delta^{18}O$) have been applied to assess the fidelity of the carbon and oxygen isotope data presented herein (see Supporting Information).

Generally, brachiopods with Mn/Ca ratio of ≤1 mmol/mol show well-preserved shell ultrastructure and usually exhibit Sr/Ca ratios ≥1.3 mmol/mol, which is comparable to values reported for well-preserved early Paleozoic biogenic calcite (C. M. Ø. Rasmussen et al., 2016; Steuber & Veizer, 2002). Therefore, these brachiopods probably represent the best-preserved samples in our data set. Importantly, the secular Ordovician carbon and oxygen isotope trend herein recorded from Öland remains unchanged whether or not only samples below a particular element/Ca ratio preservation limit (e.g., ≤1 mmol/mol Mn/Ca) are considered (Figure 10), which is similar to the conclusion reached by Veizer et al. (1999) and more recently by Goldberg et al. (2021).

6.2. Carbon Isotopes

Over the last three decades, the carbon isotope stratigraphy of Baltoscandian Ordovician successions has been extensively documented, albeit mainly based on bulk rock carbonates (e.g., Ainsaar et al., 1999, 2004, 2007, 2010; Bauert et al., 2014; Calner et al., 2014; Kaljo et al., 2007; Lindskog et al., 2019; Wu et al., 2017; Figure 11). This has enabled the identification of lower Paleozoic carbon isotope excursions which have been used as important stratigraphic correlation tools, for instance, the MDICE (Ainsaar et al., 2004, 2010, 2020; Kaljo et al., 2007; Saltzman & Edwards, 2017; Schmitz et al., 2010; Young et al., 2016). In one of the first studies to devote attention to the Early Ordovician interval in Baltoscandia, Calner et al. (2014) investigated the upper Tremadocian to middle Darriwilian $\delta^{13}C$ record of the Orthoceratite Limestone of Öland, Sweden, and made comparisons to that of the Argentine Precordillera. Although that study was not biostratigraphically constrained, a negative excursion (ca. 1‰) in the basal parts of the Köpingsklint Formation followed by a marked positive excursion was reported as potentially valuable Lower Ordovician chemostratigraphic markers. This study was later refined and updated with biostratigraphical information (Wu et al., 2017).

C. M. Ø. Rasmussen et al. (2016) reported $\delta^{18}O$ and $\delta^{13}C$ records of the Floian to mid-Darriwilian interval in eastern Baltoscandia based on bed-by-bed brachiopod samples from Russia. Subsequently, Wu et al. (2017) documented a complete record of the MDICE (rising limb, peak interval, and falling limb) and reported that it spans the *L. pseudoplanus*, *E. suecicus*, *P. serra,* and *P. anserinus* conodont zones. Thus, the Lower to Middle Ordovician carbon isotope stratigraphy of Baltoscandia is well-constrained based on bulk rock data.

In the present study, the main carbon isotope excursion, discernible in both brachiopods and bulk carbonate, is the MDICE with a magnitude of ca. 1‰ and peak values around +1.5‰ (Figure 11). The peak of this isotope event

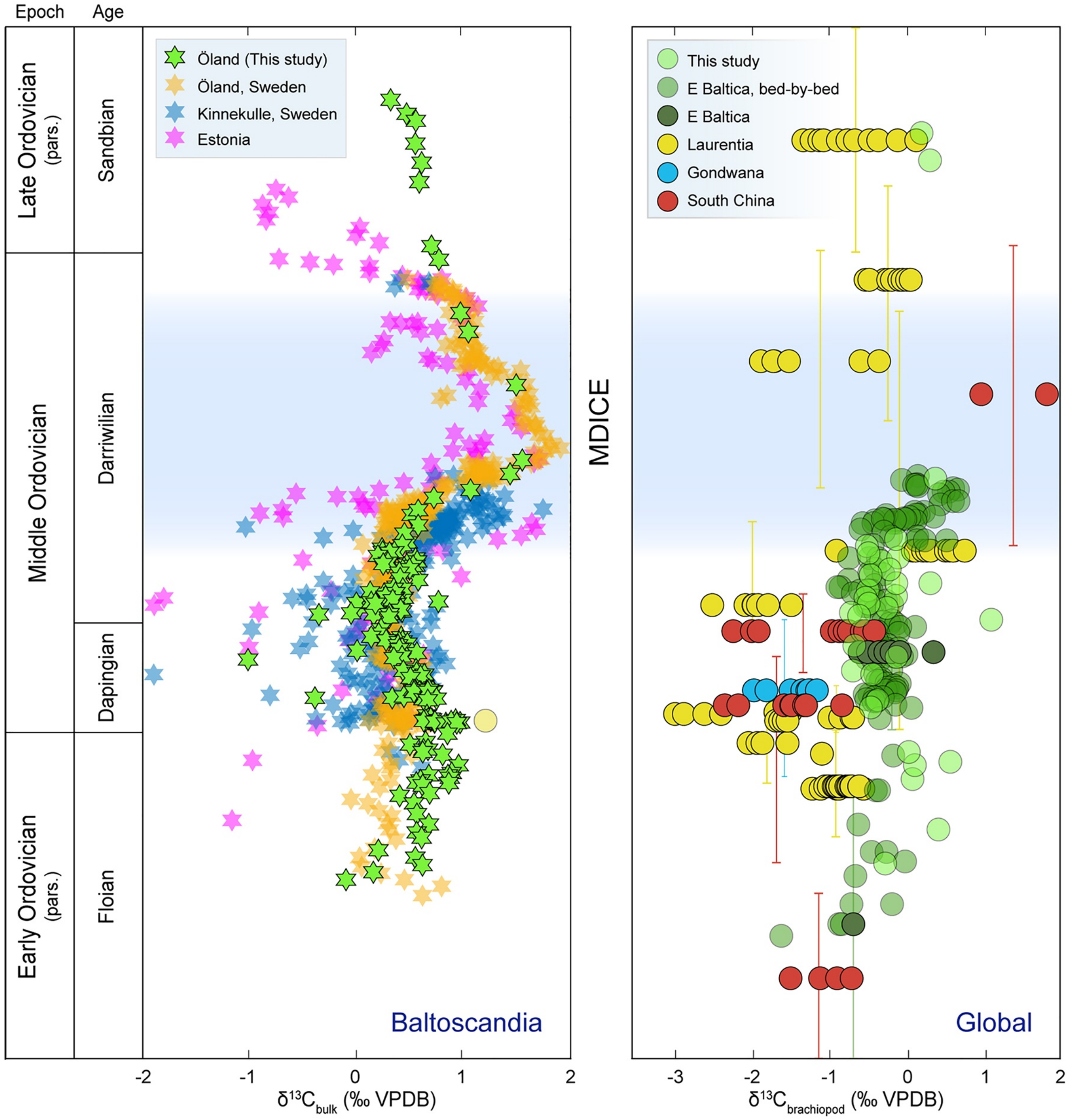

Figure 11. Comparison of regional and global whole rock carbonate and brachiopod $\delta^{13}C$ trends. Whole rock $\delta^{13}C$ data ($\delta^{13}C_{bulk}$) all originate from Baltoscandia (left figure): Öland (Wu et al., 2017); Kinnekulle (Lindskog et al., 2019); Estonia (Kaljo et al., 2007). Brachiopod $\delta^{13}C$ data (right figure) elucidate Baltoscandia $\delta^{13}C$ trends using best-preserved brachiopods (Mn/Ca ≤ 1 mmol/mol) from this study in conjunction with data from C. M. Ø. Rasmussen et al. (2016) compared to reported brachiopod $\delta^{13}C$ trends from global compilations (Qing & Veizer, 1994; Shields et al., 2003; Veizer et al., 1999; Veizer & Prokoph, 2015). Note the MDICE trend in both curves (further supported by the full Öland data set shown in Figure 10), as well as the temporal resolution of the Baltic brachiopod bed-by-bed data set as compared to the global sites. Vertical bars in the right diagram denote stratigraphical uncertainty of the global compilation samples highlighted in corresponding colors. This temporal constraint is based on either the provided lithostratigraphical information in the source references using C. M. Ø. Rasmussen et al. (2019) or biostratigraphy, based on brachiopod species ranges where possible (St. Petersburg: Egerquist (2004), Yangtze Platform: Zhan et al. (2007)).

is at −54.8 to −52.4 m of the Kårehamn core, corresponding to the *E. suecicus* Conodont Zone (Figure 10). There is overall agreement between bulk rock and brachiopod $\delta^{13}C$ trends (Figures 10 and 11), with about 0.5‰ lighter $\delta^{13}C_{brachiopod}$ values, although minor differences exist. This is consistent with observations that over specific time intervals, brachiopod and bulk rock $\delta^{13}C$ records show good correlation, but some deviations exist (Brand, 2004; Munnecke et al., 2010). One potential cause of deviations between bulk carbonate and brachiopod records may be variations in temporal and spatial resolution of these archives. Brachiopod-based isotope records may frequently suffer from limited stratigraphic resolution (Munnecke et al., 2010) which may impair their fidelity for high-resolution chemostratigraphic work. This limitation may very well explain the apparent difference in the expression of the MDICE between the paired brachiopod-bulk Baltoscandian record (Figure 11), where the higher resolution of the bulk rock record reflects an extended record of the MDICE whereas the brachiopod record reflects only the lower part of this carbon isotope excursion. Furthermore, the composite brachiopod record seems to indicate a short-term positive trend which is not reflected in the bulk rock record at the base of the MDICE interval (Figure 11). Importantly, this trend visible in the brachiopod record at the base of the MDICE interval cannot be confirmed as the East Baltic data set it is recorded in does not extend further upwards stratigraphically (e.g., C. M. Ø. Rasmussen et al., 2016) and is not present in the only other coeval brachiopod record from Baltica (i.e., the full Öland record, Figure 10). Nevertheless, while the reason for this disparity is not immediately clear, what is apparent is that a positive excursion is recorded in both bulk rocks and brachiopods during the middle Darriwilian which corresponds to the MDICE as reported by other workers (e.g., Lindskog et al., 2019; C. M. Ø. Rasmussen et al., 2016; Wu et al., 2017).

Primary inter-specific and intra-specific variability of $\delta^{13}C$ (and $\delta^{18}O$) is documented in literature for ancient (e.g., Korte et al., 2005; Korte & Hesselbo, 2011; Veizer et al., 1999) and modern brachiopods (e.g., Takayanagi et al., 2013, 2015; Ullmann et al., 2017) and are linked to pronounced seasonality of the shallow marine depositional environment, metabolism-mediated or kinetic fractionation effects (Auclair et al., 2003; Korte et al., 2005, 2017; Takayanagi et al., 2015). The smooth trend evident in the current $\delta^{13}C_{bulk}$ record can be explained by the mixing of microscopic-sized carbonate fragments in the micritic carbonates, which yield homogenized $\delta^{13}C$ compositions and consequently, generated the smoothed isotope curves that can display high-frequency $\delta^{13}C$ variability (cf. Korte et al., 2017). It is documented that carbon isotope records from epeiric sea settings may be strongly affected by local-scale carbon cycle changes (e.g., Holmden et al., 1998; Panchuk et al., 2005). Thus, it is can be expected that $\delta^{13}C$ records from these settings exhibit strong variation in contrast to the open ocean, where variations in $\delta^{13}C$ values of dissolved inorganic carbon (DIC) are relatively small (Swart et al., 2015). Consequently, the smooth trend of the Öland $\delta^{13}C_{bulk}$ record (Figure 11) potentially suggests that $\delta^{13}C$ trends characteristic of open ocean conditions may also be reflected by records originating from epicontinental sea settings.

6.2.1. Regional and Global Comparison of the Baltoscandian $\delta^{13}C$ Record

The 0.5‰ offset between $\delta^{13}C_{brachiopod}$ and $\delta^{13}C_{bulk}$ in the current study seems to be a consistent pattern throughout the Baltoscandian Paleobasin. Specifically, Floian to Sandbian $\delta^{13}C_{bulk}$ values from different parts of Baltoscandia (Figure 11) show a range between −1‰ and +2‰ (Kaljo et al., 2007; Lindskog et al., 2019; Wu et al., 2017). For fossil brachiopods, values ranging between −1‰ and +1‰ have been reported for the eastern Baltoscandian Paleobasin (e.g., Bergmann et al., 2018; C. M. Ø. Rasmussen et al., 2016) and these are comparable with our observations (Figure 6). Floian–Sandbian $\delta^{13}C_{bulk}$ range between −1.0‰ and +1.6‰, and best-preserved $\delta^{13}C_{brachiopod}$ values (with Mn/Ca ≤ 1 mmol/mol) range between −0.7‰ and +0.4‰. This offset may reflect a basin configuration where deeper waters are ^{13}C-depleted and the upper parts are ^{13}C-enriched due to the transport of organic matter to deeper waters (Kroopnick et al., 1977; van de Schootbrugge et al., 2000). However, this is unlikely to be the case as the Baltoscandian Paleobasin was characterized by very low relief (Jaanusson, 1973) and thus, no significant differences in water depth in the sea. Therefore, lighter $\delta^{13}C$ values in brachiopods compared to the bulk rock data potentially reflects species-specific vital effects (e.g., Auclair et al., 2003; Takayanagi et al., 2015).

Comparison of the new Baltic $\delta^{13}C_{brachiopod}$ record to published data and compilations (Shields et al., 2003; Veizer et al., 1999; Figure 11) reveals that the Baltoscandian record is characterized by generally heavier $\delta^{13}C_{brachiopod}$ values. This disparity can be attributed to local/regional differences in C isotope compositions, and this is in concert with data from several other sedimentary basins (Shields et al., 2003; Veizer et al., 1999) which have depositional environments and tectonic regimes different from those of the Baltoscandian Paleobasin (see Supporting Information). Nevertheless, the apparent similarity in the trends of both $\delta^{13}C_{brachiopod}$ records strengthens the view that the Baltoscandian $\delta^{13}C_{brachiopod}$ reflects a near-primary record and a global trend.

6.3. Oxygen Isotopes

The composite Baltic $\delta^{18}O$ record (Figure 12) reveals a secular Floian to Sandbian $\delta^{18}O$ increase of ca. 1.4‰. This is most apparent during the Darriwilian, where an increase of ca. 0.5‰–0.8‰ is recorded within the well-preserved samples (Figure 10), mirroring the Lower to Middle Ordovician $\delta^{18}O_{brachiopod}$ trend from east-

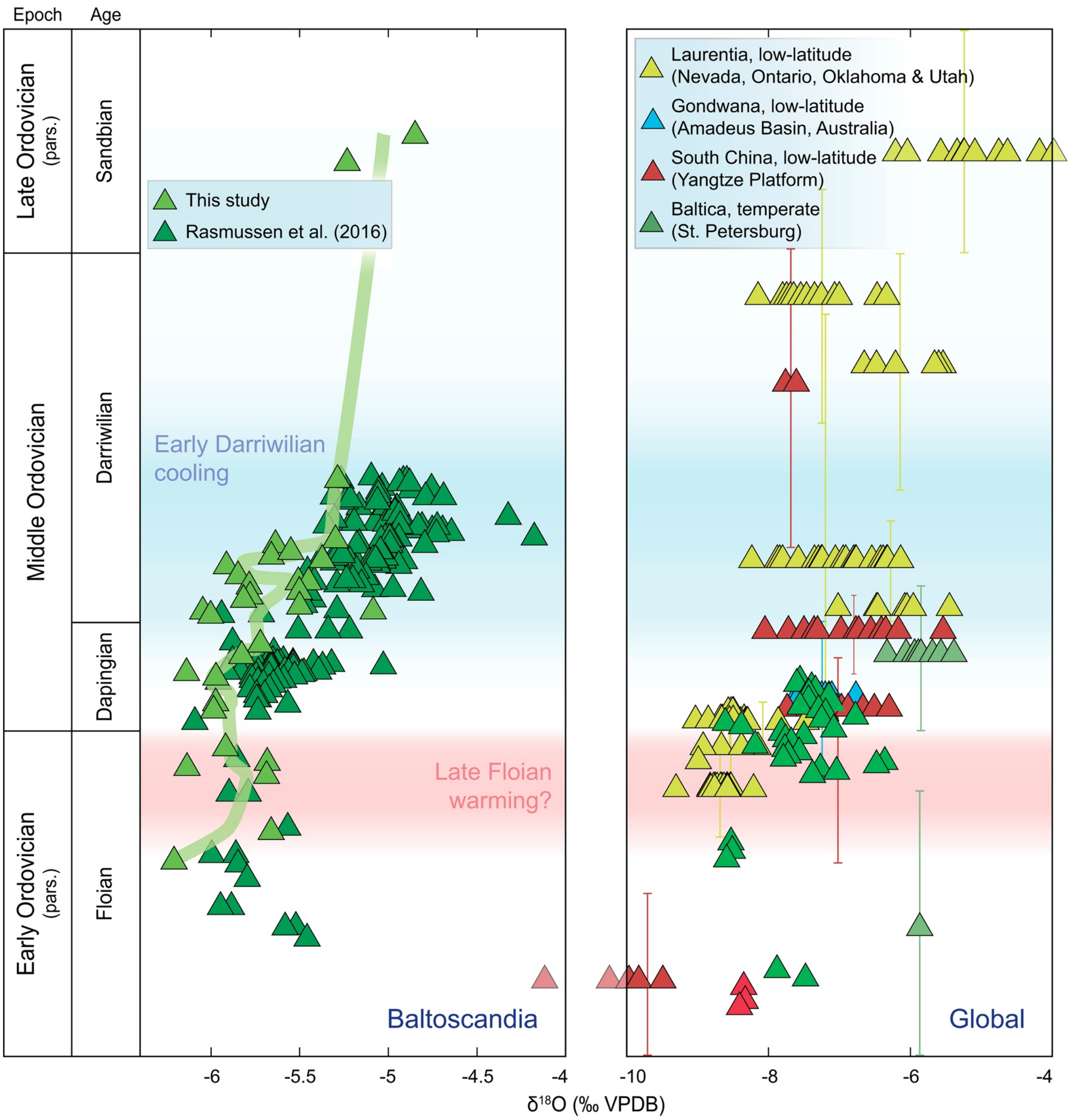

Figure 12. Long-term comparison between Early Ordovician (Floian) to early Late Ordovician (Sandbian) brachiopod $\delta^{18}O$ values in Baltoscandia (based on pristine brachiopods) and global brachiopod $\delta^{18}O$ compilations. Both the Baltoscandian and global compilation data sets elucidate a general pattern of increasing brachiopod $\delta^{18}O$ values upwards, which is most prominent during the Middle Ordovician (compare with Figure 2 showing a similar trend based on published clumped isotope data sets. A five-point LOWESS smoothing has been added to the Öland data set to accentuate the temporal trends using the software OriginPro. Colored vertical bars in the right diagram denote stratigraphical uncertainty of the global compilation samples highlighted in corresponding shades. Note the well-resolved temporal resolution of the Baltic brachiopod bed-by-bed data set as compared to the global data points. Global compilation data set obtained from Qing and Veizer (1994), Veizer et al. (1999), Shields et al. (2003), and Veizer and Prokoph (2015). Samples are temporally constrained as in Figure 11.

ern Baltoscandia (C. M. Ø. Rasmussen et al., 2016; Figure 12). The similarity between these oxygen isotope records (Figure 12) thus suggests that the Baltoscandian Lower to Middle Ordovician oxygen isotope record is spatially consistent and a primary geochemical signature. We note, however, that an offset of ca. 0.6‰ is apparent between the Öland and Russia data set. Although a systematic taxonomic identification was not conducted before geochemical analyses of brachiopod fossils, this offset may be due to potential species-specific or specimen-specific vital effects (e.g., Korte et al., 2017; Takayanagi et al., 2015) between the different brachiopod species analyzed from the two localities. Alternatively, it may reflect local variability in freshwater input or variable

10.1029/2021PA004309

fossil brachiopod preservation within the paleobasin. Nevertheless, the similarity of the brachiopod δ^{18}O trends is striking, regardless of the reason for the apparent offset, and this is our main focus.

Although the upper Darriwilian to Sandbian portion of the Baltic δ^{18}O record is less constrained, data from the best-preserved brachiopods suggests that δ^{18}O values in that period remained at least as heavy as during middle Darriwilian times. This is congruent with published records indicating a transient cooling event at this time (Saltzman & Young, 2005; Vandenbroucke, Armstrong, Williams, Paris, Zalasiewicz, et al., 2010). Furthermore, the Early to Late Ordovician Baltoscandian δ^{18}O record of the present data set is consistent with the trend of increasing δ^{18}O values with decreasing age, and this has long been documented for the Ordovician (Grossman & Joachimski, 2020; Qing & Veizer, 1994; Shields et al., 2003; Veizer et al., 1999; Veizer & Prokoph, 2015). However, the current Baltic data set provides improved temporal resolution compared to the global compilations, which have limited resolution in the Ordovician (see Figure 12 for comparison of data sets).

6.3.1. Regional and Global Comparison of the Baltoscandian δ^{18}O Record

The comparison of the Baltoscandian δ^{18}O record with global compilation data (Figure 12) indicates that the Baltoscandian record is characterized by heavier δ^{18}O values. This may be attributable to the paleogeographical position of Baltica during the studied interval, as well as the relatively shallow sedimentary burial—thus, reduced susceptibility to burial diagenesis—which largely characterized the Baltoscandian Paleobasin. The mid latitudinal positions, which Baltica occupied during the Early to Middle Ordovician (Torsvik et al., 2012) suggests that Baltoscandian brachiopods lived in cooler seawater compared to their counterparts in more equatorial paleocontinents (and thus, warmer paleoclimates), which constitute the majority of the Ordovician global compilation data (Shields et al., 2003; Veizer et al., 1999; Figure 12). For instance, the paleocontinent of Laurentia was in equatorial realms throughout the Ordovician while Baltica only approached equatorial paleolatitudes during the Late Ordovician (Kaljo et al., 2007). It is important to note that the global δ^{18}O compilation data (Figure 12) was measured from brachiopod fossils from diverse localities with different depositional contexts including different depositional and burial histories, all of which may have potentially had an influence on the δ^{18}O values measured from these specimens. However, since these global compilation data represent the best-preserved data set from these diverse localities (Qing & Veizer, 1994; Shields et al., 2003; Veizer et al., 1999), it is reasonable to consider that the δ^{18}O offset between these low-latitude sites and Baltica (Figure 12) signifies the presence of a latitudinal seawater temperature gradient during the Ordovician. This is congruent with previous suggestions of a latitudinal temperature gradient during the Ordovician based on paleontological data (e.g., Vandenbroucke, Armstrong, Williams, Paris, Sabbe, et al., 2010).

6.4. Paleoenvironmental Significance of the Baltoscandian Oxygen Isotope Record

Temporal variation in δ^{18}O of biogenic calcite can be influenced by several factors including changes in seawater δ^{18}O composition, temperature of calcite precipitation, vital effects, pH changes, and diagenetic alteration of near-primary brachiopod δ^{18}O (Bruckschen & Veizer, 1997; Munnecke et al., 2010; Qing & Veizer, 1994; Swart, 2015). Climatic cooling has been invoked as an explanation for the Ordovician δ^{18}O trend observed in both brachiopods and conodonts, and cooling, in turn, has been associated with the coinciding GOBE (Qing & Veizer, 1994; C. M. Ø. Rasmussen et al., 2016; Trotter et al., 2008). Alternative interpretations have also been postulated for this trend including changes in the oxygen isotope composition of seawater (Jaffrés et al., 2007; Shields et al., 2003) and diagenetic alteration (Bergmann et al., 2018).

In the current Baltoscandia record, vital effects are unlikely to explain the secular δ^{18}O trend because the secondary layer of brachiopod shells, which are more likely to have been secreted in isotopic equilibrium with or very close to the seawater, were utilized (Carpenter & Lohmann, 1995; Ullmann et al., 2017). Although the δ^{18}O values during the lower Darriwilian and upper Darriwilian to upper Sandbian portion of the Öland data show a wide range (Figure 10) suggesting that diagenesis has modified some of the primary δ^{18}O compositions, the best-preserved samples (Figures 10 and 12), however, show a long-term trend which is consistent with the δ^{18}O LOWESS smoothing line and narrow δ^{18}O range (Figure 10), indicating that the near-primary δ^{18}O trends are preserved (see also Section 6.1).

Besides the influence of significant ice-volume changes, seawater δ^{18}O composition may become heavier through high-temperature reactions of seawater with silicate minerals in hydrothermal systems associated with oceanic

10.1029/2021PA004309

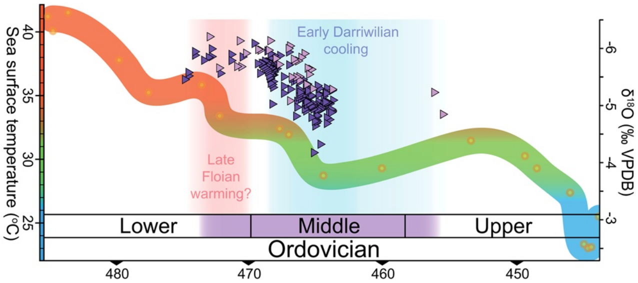

Figure 13. Comparison of the current study's brachiopod derived ^{18}O-data to the apatite ^{18}O-clumped isotope curve of Trotter et al. (2008). Note the parallel trend of increasing oxygen isotope values through the lower Middle Ordovician.

ridges and their flanks (Veizer & Prokoph, 2015; Verard & Veizer, 2019, and references therein). Results based on modeling efforts show that the maximum rate of change of the δ^{18}O composition of seawater due to high-temperature reactions is ca. 1‰ per 100 million years (Jaffrés et al., 2007; Veizer & Prokoph, 2015). However, the time period covered by the current Baltic data set is ca. 19 million years (Gradstein & Ogg, 2020), thus making it unlikely that seawater-silicate rock interactions could have been rapid enough to generate the observed δ^{18}O change. Furthermore, clumped isotope results based on Middle Ordovician brachiopods have been reported to yield seawater δ^{18}O compositions between −0.9‰ and −1.2‰ (Bergmann et al., 2018), and this is comparable to δ^{18}O compositions of modern seawater.

Consequently, we interpret the long-term Baltoscandia $\delta^{18}O_{brachiopod}$ trend as dominantly reflecting a near-primary paleotemperature signal, in agreement with previous studies (Goldberg et al., 2021; C. M. Ø. Rasmussen et al., 2016; Trotter et al., 2008). In this scenario, the δ^{18}O trend represents a transition from warmer climatic conditions during the Early Ordovician to less-warm conditions during the Early to Middle Ordovician transition and a cooling episode during the Darriwilian which may have persisted into the Sandbian (Figure 13).

6.4.1. Middle Ordovician Cooling

The composite Baltoscandia record (Figure 12) indicates a ca. 0.8‰–1.5‰ $\delta^{18}O_{brachiopod}$ increase between the Floian and mid-Darriwilian. Assuming a ~4°C temperature change for 1‰ δ^{18}O shift (Epstein & Mayeda, 1953), this is suggestive of a ca. 3–6°C relative cooling within a period of ca. 8 million years (Gradstein & Ogg, 2020) if an ice-free world even during the period with cooler temperatures is assumed (Gradstein & Ogg, 2020). This relative cooling estimate is comparable to bio-apatite-based and brachiopod-based estimates of sea surface temperature evolution during the same interval (Goldberg et al., 2021; Grossman & Joachimski, 2020; Trotter et al., 2008). The northward drift of Baltica from temperate southerly latitudes toward the equator during the Ordovician (Torsvik & Cocks, 2019; Torsvik et al., 2012) can be expected to have resulted in progressively lighter brachiopod δ^{18}O values due to warmer equatorial temperatures as Baltica progressively moved toward the sub-tropics. However, the opposite trend is apparent in the δ^{18}O record. Therefore, the 0.8–1.5‰ amplitude of change in $\delta^{18}O_{brachiopod}$ potentially represents an underestimation of the actual global seawater temperature change. Moreover, short-term sea-level fall occurs in the upper part of the Dapingian, and a pronounced and long-lasting sea-level fall is observed both at the regional and global scale starting within the lowermost Darriwilian, suggesting a good correspondence with the pronounced shift to heavier δ^{18}O values during the Middle Ordovician (Figure 14). These observations support glacio-eustasy driven by climatic cooling and this would suggest that a portion of the $\delta^{18}O_{brachiopod}$ increase is related to the ice volume effect and the temperature decline on Baltica was less than 3–6°C.

Biofacies analyses of brachiopods, conodonts, and trilobites have all demonstrated that shallow-water faunas became ubiquitous in Baltoscandia during the lower Darriwilian, indicative of falling sea level in the order of 150 m from the upper Floian to the lower Darriwilian (Nielsen, 1995; C. M. Ø. Rasmussen et al., 2016; J. A. Rasmussen & Stouge, 2018; Stouge et al., 2020). Also, before the Middle Ordovician, lighter $\delta^{18}O_{brachiopod}$ values during the upper Floian (Figure 12) coincide with the late Floian migration of Laurentian warm-water conodont taxa into Baltoscandia (i.e., an influx of species typical of low-latitude regions), interpreted to denote a relatively brief warming episode. Hereafter follows the Middle Ordovician influx of temperate-water taxa denoting cooler waters (Bagnoli & Stouge, 1997; Stouge et al., 2020).

In addition to paleontological evidence, several sedimentological, sequence- and cyclostratigraphical studies have argued for global lower Darriwilian cooling that likely transgressed into the Sandbian. In Baltica, detailed lithofacies and microfacies analyses on lowermost Darriwilian carbonates corroborate this view (Lindström, 1984; Lindskog et al., 2019) and so does sequence stratigraphical evidence from Armorica (Dabard et al., 2015). In Siberia, a sudden shift from continuous deposition of warm-water carbonates to the lower−middle Darriwilian Baykit Sandstone is seen in the Tunguska Basin. The base of this up to 80 m thick sandstone succession represents one of the largest unconformities on the Siberian Platform and is believed to reflect a major forced

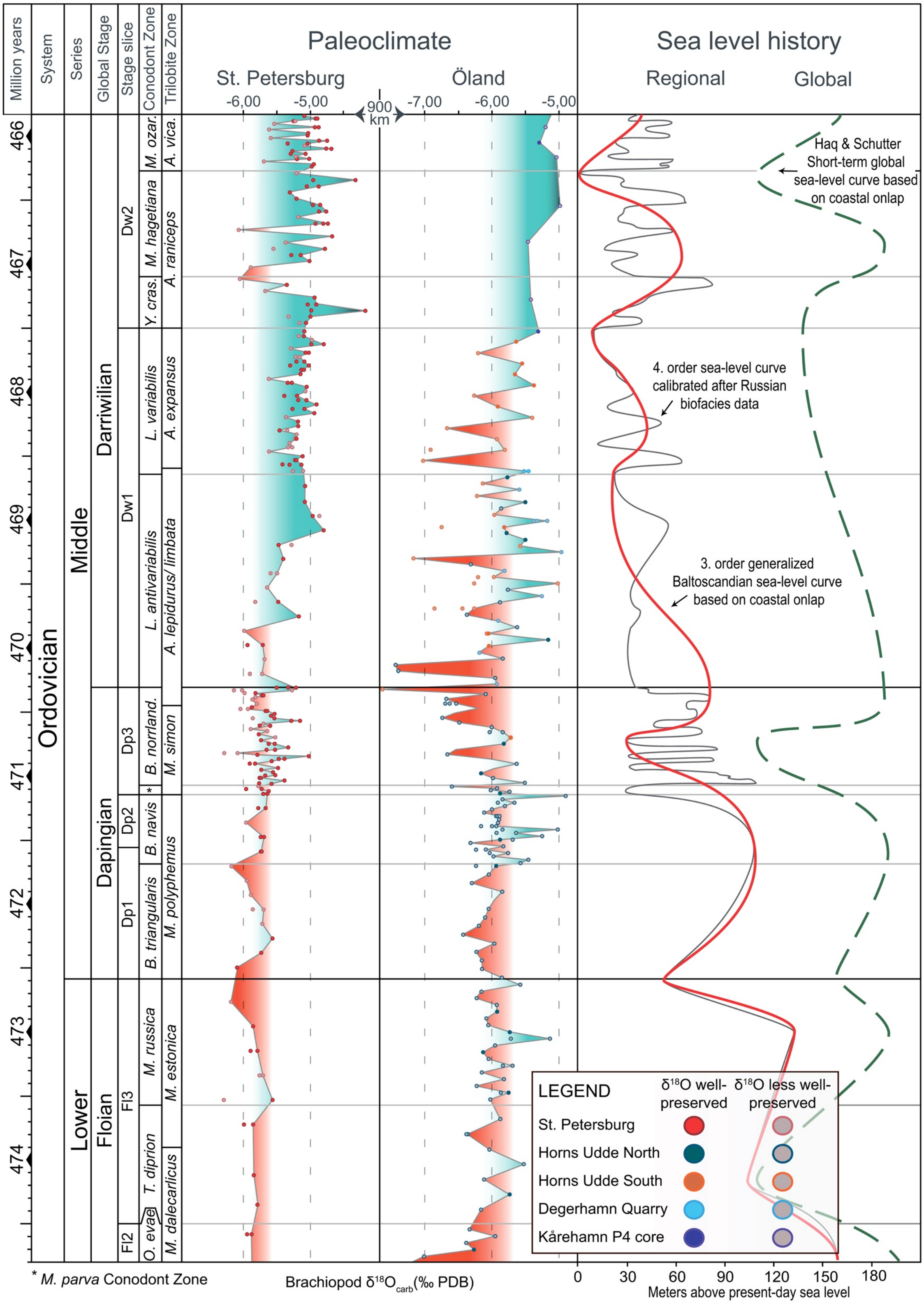

Figure 14. Middle Ordovician $\delta^{18}O_{brachiopod}$ and sea level evolution across the Baltoscandian Paleobasin. Note that even though the fourth-order sea-level curve (right) is based on a biofacies framework from the St. Petersburg region, individual excursions in the δ^{18}O-Öland curve are still mirrored. δ^{18}O-St. Petersburg curve and sea-level curves as in C. M. Ø. Rasmussen et al. (2016) but here calibrated to the time domain. Original sea level data modified from Hansen and Nielsen (2003), Haq and Schutter (2008), Nielsen (1995, 2004, 2011), and C. M. Ø. Rasmussen et al. (2009).

regression (Kanygin et al., 2010). A similar major regressional phase is seen in Laurentia, represented by the Dapingian−lower Darriwilian Knox Unconformity which may be up to 10 million years long or more (Pope & Read, 1998; Ross & Ross, 1992, 1995). In the upper parts of the Darriwilian−lower Sandbian, sequence stratigraphical and lithological evidence from eastern Laurentia suggests a shift to cooler climate as witnessed by the transition from tropical to temperate carbonates believed to be associated with either the Taconic Orogeny (Holland & Patskowsky, 1996, 1998), or globally cooling climate (Lavoie, 1995; Pope & Read, 1998). Direct near-field Gondwanan evidence for glaciations has not been documented lithologically. Indirectly, however, evidence comes from sequence stratigraphical packages inferred to reflect glacio-eustacy. Turner et al. (2011) showed that an intricate third-order regressive-transgressive sequence stacking pattern was in place already by the Early Ordovician in the Cape Peninsula in South Africa which was situated at subtropical to mid-latitudes at that time. More near-field at higher latitudes in Gondwana, Turner et al. (2012) presented indirect evidence from Jordan in the form of third- and fourth-order sequence stratigraphical packages through the Darriwilian–Sandbian that was inferred to be glacio-eustatic in origin. Finally, cyclostratigraphical evidence has been used to infer that the MDICE-interval is associated with falling sea level on Baltica (Cherns et al., 2013) and on the Tarim Block (Fang et al., 2019). Most recently, J. A. Rasmussen et al. (2021) used a marginal succession on Baltica to show a shift in the expression of orbital cycles that postdates by just 200,000 years the brachiopod ^{18}O-inferred onset of colder climate in the upper *B. norrlandicus* zone. This orbital shift was suggested to be associated with the build-up of icecaps in Gondwana.

In summary, therefore, the discussion of whether the Middle Ordovician oxygen isotope trend is climate-related, or reflecting either diagenetic overprint (Bergmann et al., 2018) or changing seawater composition (Veizer & Prokoph, 2015) seems to overlook the point that climate is invoked as a main driver for this secular trend based on a whole suite of *other* proxies found globally that independently from the oxygen isotope record indicate sea-level fluctuations, and, in many cases, on a bed-by-bed scale (Figure 14). Of equal importance is the rapidity of these sea-level oscillations such as those observed in the upper Dapingian and in the *L. variabilis*−*Y. crassus* interval of the Darriwilian. As they occur in a stable intra-cratonic setting on Baltica, it is difficult to invoke other causal mechanisms than glacio-eustasy. We note, however, that high-frequency fluctuations in fourth-order sea-level changes are only expressed in the upper Dapingian and then again in the *L. variabilis* Zone to the *M. ozarkodella* Conodont subzone of the Darriwilian (Figure 14). Perhaps, this change in the expression of sea-level change is linked to distinct phases of ice-sheet growth, with high-frequency fluctuations particularly well-expressed in an upper Dapingian phase that saw the onset of growth of continental ice with small volume ice-changes paced by orbital changes. The *L. antivariabilis* Zone, instead, may have been characterized by the establishment of a larger but stable ice sheet, less sensitive to high-frequency fluctuations. The return to more prominent high-frequency fluctuations in fourth-order sea-level changes in the *L. variabilis* Zone, and within the rest of the studied succession, could be due to the third phase of ice-sheet growth with a new increase in volume of continental ice occupying new areas that were particularly sensitive to ice growth and decay via orbital changes. Although this interpretation is highly speculative, it presents the merit to reconcile observed trends in sea-level change and $\delta^{18}O_{brachiopod}$ data.

A similar interpretation was suggested based on a sequence stratigraphical analysis of lower Darriwilian sections from southern Jordan (Turner et al., 2012), as did model simulations which suggest that the climatic threshold for glacial onset was reached during the Darriwilian (Pohl et al., 2016 and references therein), in agreement with reported contemporaneous third-order eustatic cycles.

6.4.2. Deciphering Orders of Sea-Level Change

In successions lacking a properly calibrated astrochronological framework—something still in its infancy when it comes to early Paleozoic rocks—only a high-resolution sequence- or ecostratigraphical analysis can usually resolve sea-level changes at a sufficient temporal resolution to recognize glacio-eustasy. This has been done, in detail, on lowermost Darriwilian rocks of Baltica (Nielsen, 1995; C. M. Ø. Rasmussen et al., 2009, 2016) and Armorica (Dabard et al., 2015), revealing similar magnitude third-order sea-level oscillations potentially at the kyr-scale. The millennial-scale of the sea-level changes on Baltica was recently confirmed by a geochronologically calibrated astrochronology through the Dapingian−early Darriwilian (J. A. Rasmussen et al., 2021) further supporting the notion that they are glacio-eustatically controlled. This interval precisely correlates to the interval where the current Baltic $\delta^{18}O$ record shows the strongest positive trend, in accordance with the inferred lower Middle Ordovician sea-level drop (Figure 14).

The trend toward relatively heavier upper Darriwilian−Sandbian brachiopod $\delta^{18}O$ values reported here occurs at the start of an interval where global and regional sea-level estimates suggest the start of a sea-level rise that eventually peaked during the early−mid Katian (Hallam, 1992; Haq & Schutter, 2008; Nielsen, 2004; C. M. Ø. Rasmussen et al., 2019). This, therefore, seems to oppose a climatic driver for the oxygen isotope trend in this interval. However, as with the early Darriwilian (where there is a discordance between the actual brachiopod $\delta^{18}O$ trend and the expected trend based on the paleolatitudinal location of Baltica), there is a discordance between the $\delta^{18}O$-signal and inferred eustatic sea-level rise during the later Darriwilian−Sandbian times as the latter would suggest a warming pulse.

It is therefore expedient to distinguish between first-order plate tectonic-induced changes and the dramatic amplitudes of third- and fourth-order sea-level changes suggestive of the waxing and waning of ice sheets (Hallam, 1992; Haq & Schutter, 2008; Nielsen, 2004, 2011). Whereas climatic cooling likely accelerated faster than the expected latitudinal temperature gradient during the early Darriwilian, the first-order sea level rise may have subsequently outpaced the third-order sea-level fall from the later Darriwilian onwards.

7. Conclusions

This study presents biostratigraphically well-resolved brachiopod and bulk carbonate carbon and oxygen isotope data spanning the Lower (Floian) to lower Upper Ordovician (Sandbian) of Baltoscandia. The temporal scale of this Baltoscandian data set allows for considerable refinement from a midlatitude perspective of previously published global carbon and oxygen isotope data, which historically have been characterized by spot sampling across several paleoplates in low-latitude settings.

Several lines of evidence indicate that, while the carbon and oxygen isotope data set may have been affected by diagenetic alteration, long-term trends in isotopic compositions which are useful for paleoenvironmental interpretation, are preserved. Our $\delta^{18}O$ record from Öland reveals that previously reported Lower to Middle Ordovician $\delta^{18}O$ trends from eastern Baltoscandia are spatially consistent and together, the composite Baltoscandian $\delta^{18}O$ record is concordant with global Ordovician $\delta^{18}O$ compilations, which show a Lower to Upper Ordovician $\delta^{18}O$ increasing trend. We interpret the Baltoscandian $\delta^{18}O$ record as being dominated by a paleotemperature signal indicating a transition from warmer paleotemperatures during the Lower Ordovician to cooler conditions in the Middle Ordovician.

Thus, the Baltoscandian $\delta^{18}O$ record is compatible with previous studies which suggest that present-day seawater temperatures were attained during the Darriwilian. This optimal temperature window may have sparked the GOBE.

Data Availability Statement

The data set associated with the current study can be found at University of Copenhagen's Electronic Research Data Archive (ERDA) at https://doi.org/10.17894/ucph.546c77e7-9899-4e66-b2d0-944fcf54a580. The paleothermometry trend depicted in Figure 2 is based on ^{18}O-conodont apatite from Trotter et al. (2008) and ^{18}O-bulk rock data from Goldberg et al., 2021. The Trotter et al. (2008) data set is also used in Figure 13. The global $\delta^{13}C$ and ^{18}O data shown in Figures 11 and 12 are based on data sets from Qing and Veizer (1994), Shields et al. (2003), Veizer et al. (1999), Veizer and Prokoph (2015), and C. M. Ø. Rasmussen et al. (2016). Original sea level data in Figure 14 is modified from Hansen and Nielsen (2003), Haq and Schutter (2008), Nielsen (1995, 2004, 2011) and C. M. Ø. Rasmussen et al. (2009). ^{18}O data from western Russia is based on C. M. Ø. Rasmussen et al. (2016).

Acknowledgments
The authors acknowledge Bo Petersen for help with isotope analysis, Laurent Nicod, and Claudia Baumgartner (UNIL) for help with thin-section preparation. Morten L. Nielsen, Bristol, is thanked for field assistance, as are Cementa, the company operating the Degerhamn quarry, who permitted us to collect samples, and Länsstyrelsen in Kalmar who gave permission to GB and SS to sample the sections at Horns Udde. The study was funded by GeoCenter Denmark Grant nos. 2015-5 and 3-2017 to CMØR. This study is a contribution to IGCP project 735 − "Rocks and the Rise of Ordovician Life (Rocks n' ROL)"

References

Ainsaar, L., Kaljo, D., Martma, T., Meidla, T., Männik, P., Nõlvak, J., & Tinn, O. (2010). Middle and upper Ordovician carbon isotope chemostratigraphy in Baltoscandia: A correlation standard and clues to environmental histor. *Palaeogeography, Palaeoclimatology, Palaeoecology*, *294*(3–4), 189–201. https://doi.org/10.1016/j.palaeo.2010.01.003

Ainsaar, L., Meidla, T., & Martma, T. (1999). Evidence for a widespread carbon isotopic event associated with late Middle Ordovician sedimentological and faunal changes in Estonia. *Geological Magazine*, *136*, 49–62. https://doi.org/10.1017/s001675689900223x

Ainsaar, L., Meidla, T., & Tinn, O. (2004). Middle and upper Ordovician stable isotope stratigraphy across the facies belts in the East Baltic. *Paper presented at the Proceedings WOGOGOB-2004 Conference materials, Tartu, 2004*.

Ainsaar, L., Tinn, O., Dronov, A. V., Kiipli, E., Radzevicius, S., & Meidla, T. (2020). Stratigraphy and facies differences of the Middle Darriwilian isotopic carbon excursion (MDICE) in Baltoscandia. *Estonian Journal of Earth Sciences*, *69*(4), 214–222. https://doi.org/10.3176/earth.2020.16

Auclair, A.-C., Joachimski, M. M., & Lécuyer, C. (2003). Deciphering kinetic, metabolic and environmental controls on stable isotope fractionations between seawater and the shell of *Terebratalia transversa* (Brachiopoda). *Chemical Geology*, *202*(1–2), 59–78. https://doi.org/10.1016/s0009-2541(03)00233-x

Bagnoli, G., & Stouge, S. (1996). Changes in conodont provincialism and biofacies during the lower Ordovician in Öland, Sweden. *Palaeopelagoes*, *6*, 19–29.

Bagnoli, G., & Stouge, S. (1997). Lower Ordovician (Billingenian–Kunda) conodont zonation and provinces based on sections from Horns Udde, north Öland, Sweden. *Bolletino della Societa Paleontologica Italiana*, *35*, 109–163.

Bagnoli, G., & Stouge, S. (1999). Bentonite beds and discontinuity surfaces as correlative tools in the Lower Ordovician carbonates of Baltoscandia. In A.Farinacci, & A. R.Lord (Eds.), *Depositional episodes and bioevents* (pp. 29–38).

Barnes, C. R. (2004). *Ordovician oceans and climate: The Great Ordovician Biodiversification Event*, 72–76. https://doi.org/10.7312/webb12678-008

Bauert, H., Ainsaar, L., Poldsaar, K. & Sepp, S. (2014). δ13C chemostratigraphy of the middle and Upper Ordovician succession in the Tartu 453 drillcore, Southern Estonia, and the significance of the HICE. *Estonian Journal of Earth Sciences*, *63*, 195–200.

Bergmann, K. D., Finnegan, S., Creel, R., Eiler, J. M., Hughes, N. C., Popov, L. E., & Fischer, W. W. (2018). A paired apatite and calcite clumped isotope thermometry approach to estimating Cambro–Ordovician seawater temperatures and isotopic composition. *Geochimica et Cosmochimica Acta*, *224*, 18–41. https://doi.org/10.1016/j.gca.2017.11.015

Bergström, S. M. (1971). Conodont biostratigraphy of the Middle and Upper Ordovician of Europe and eastern North America. *Geological Society of America Memoir*, *127*, 83–161.

Bergström, S. M. (1980). Conodonts as paleotemperature tools in Ordovician rocks of the Caledonides and adjacent areas in Scandinavia and the British Isles. *Geologiska Foreningens I Stockholm Forhandlingar*, *102*(4), 377–392.

Bergström, S. M. (2007). The Ordovician conodont biostratigraphy in the Siljan region, south-central Sweden: A brief review of an international reference standard. *Paper presented at the 9th Meeting of the Working Group on Ordovician Geology of Baltoscandia (WOGOGOB), Field Guide and Abstracts*.

Bergström, S. M., Chen, X., Gutiérrez-Marco, J. C., & Dronov, A. (2009). The new chronostratigraphic classification of the Ordovician System and its relations to major regional series and stages and to δ^{13}C chemostratigraphy. *Lethaia*, *42*, 97–107.

Bergström, S. M., Saltzman, M. R., Leslie, S. A., Ferretti, A., & Young, S. A. (2015). Trans-Atlantic application of the Baltic Middle and Upper Ordovician carbon isotope zonation. *Estonian Journal of Earth Sciences*, *64*(1), 8–12. https://doi.org/10.3176/earth.2015.02

Bohlin, B. (1949). The Asaphus limestone of Northernmost Öland. *Bulletin of the Geological Institutions of the University of Uppsala*, *33*, 529–570.

Bohlin, B. (1953). The Lower Ordovician limestone between the Ceratopyge shale and the Platyurus limestone of Böda hamn. *Bulletin of the Geological Institution of the University of Upsala*, *35*, 111–151.

Brand, U. (2004). Carbon, oxygen and strontium isotopes in Paleozoic carbonate components: An evaluation of original seawater-chemistry proxies. *Chemical Geology*, *204*(1), 23–44. https://doi.org/10.1016/j.chemgeo.2003.10.013

Bruckschen, P., & Veizer, J. (1997). Oxygen and carbon isotopic composition of Dinantian brachiopods: Paleoenvironmental implications for the Lower Carboniferous of western Europe. *Palaeogeography, Palaeoclimatology, Palaeoecology*, *132*(1–4), 243–264. https://doi.org/10.1016/s0031-0182(97)00066-7

Calner, M., Lehnert, O., Rongchang, W., Dahlqvist, P., & Joachimski, M. M. (2014). δ13C chemostratigraphy in Lower-Middle Ordovician succession of Öland (Sweden) and the global significance of the MDICE. *GFF*, *136*(1), 48–54. https://doi.org/10.1080/11035897.2014.901409

Cárdenas, A. L., & Harries, P. J. (2010). Effect of nutrient availability on marine origination rates throughout the Phanerozoic eon. *Nature Geoscience*, *3*(6), 430–434.

Carpenter, S. J., & Lohmann, K. C. (1995). δ 18O and δ 13C values of modern brachiopod shells. *Geochimica et Cosmochimica Acta*, *59*, 3749–3764. https://doi.org/10.1016/0016-7037(95)00291-7

Chen, J., & Lindstrom, M. (1991). Cephalopod septal strength indices (SSI) and depositional depth of Swedish Orthoceratite limestone. *Geologica et Paleontologica*, *25*, 5–18.

Cherns, L., Wheeley, J. R., Popov, L., Pour, M. G., Owens, R., & Hemsley, A. R. (2013). Long-period orbital climate forcing in the early Palaeozoic? *Journal of the Geological Society*, *170*(5), 707–710. https://doi.org/10.1144/jgs2012-122

Clarke, A. (2014). The thermal limits to life on Earth. *International Journal of Astrobiology*, *13*(2). https://doi.org/10.1017/S1473550413000438

Cocks, L. R. M., & Torsvik, T. H. (2005). Baltica from the late Precambrian to the mid-Palaeozoic times: The gain and loss of a terrane's identity. *Earth-Science Reviews*, *72*, 39–66. https://doi.org/10.1016/j.earscirev.2005.04.001

Dabard, M. P., Loi, A., Paris, F., Ghienne, J. F., Pistis, M., & Vidal, M. (2015). Sea-level curve for the Middle to early Late Ordovician in the Armorican Massif (western France): Icehouse third-order glacio-eustatic cycles. *Palaeogeography, Palaeoclimatology, Palaeoecology*, *436*, 96–111. https://doi.org/10.1016/j.palaeo.2015.06.038

Dronov, A., & Rozhnov, S. (2007). Climatic changes in the Baltoscandian Basin during the Ordovician: Sedimentological and Palaeontological aspects. *Acta Palaeontologica Sinica*, *46*, S108–S113.

Dronov, A.V, Ainsaar, L., Kaljo, D., Meidla, T., Saadre, T., & Einasto, R. (2011). Ordovician of Baltoscandia: Facies, sequences and sealevel changes. In J. C.Gutiérrez-Marco, I.Rábano, & D.Garcia-Bellido (Eds.), *Ordovician of the World*. (Vol. 14, pp. 143–150). Publicaciones del Instituto Geológico y Minero de España, Cuadernos del Museo Geominero.

Edwards, C. T., Saltzman, M. R., Royer, D., & Fike, D. A. (2017). Oxygenation as a driver of the Great Ordovician biodiversification event. *Nature Geoscience*, *10*, 925–929. https://doi.org/10.1038/s41561-017-0006-3

Egerquist, E. (2004). *Ordovician (Billingen and Volkhov stages) brachiopod faunas of the East Baltic*. (PhD). Uppsala University.

Ekdale, A. A., Benner, J. S., Bromley, R. G., & deGibert, J. M. (2002). Bioerosion of lower Ordovician hardgrounds in southern Scandinavia and western north America. *Acta Geologica Hispanica*, *37*, 9–13.

Ekdale, A. A., & Bromley, R. G. (2001). Bioerosional innovation for living in carbonate hardgrounds in the Early Ordovician of Sweden. *Lethaia*, *34*(1), 1–12. https://doi.org/10.1080/002411601300068152

Epstein, S. & Mayeda, T. (1953). Variation of O^{18} content of waters from natural sources. *Geochimica et Cosmochimica Acta*, *4*, 213–224. https://doi.org/10.1016/0016-7037(53)90051-9

Eriksson, M. E., Lindskog, A., Calner, M., Mellgren, J. I. S., Bergström, S. M., Terfelt, F., & Schmitz, B. (2012). Biotic dynamics and carbonate microfacies of the conspicuous Darriwilian (Middle Ordovician) 'Täljsten' interval, south-central Sweden. *Palaeogeography, Palaeoclimatology, Palaeoecology*, *367–368*, 89–103. https://doi.org/10.1016/j.palaeo.2012.02.012

Fang, Q., Wu, H., Wang, X., Yang, T., Li, H., & Zhang, S. (2019). An astronomically forced cooling event during the Middle Ordovician. *Global and Planetary Change*, *173*, 96–108. https://doi.org/10.1016/j.gloplacha.2018.12.010

Finnegan, S., Bergmann, K., Eiler, J. M., Jones, D. S., Fike, D. A., Eisenman, I., et al. (2011). The magnitude and duration of Late Ordovician–Early Silurian glaciation. *Science*, *331*, 903–906. https://doi.org/10.1126/science.1200803

Fortey, R. A., & Cocks, L. R. M. (2005). Late Ordovician global warming – The Boda event. *Geology*, *33*, 405–408. https://doi.org/10.1130/g21180.1

Ghobadi Pour, M., Williams, M., & Popov, L. E. (2007). A new Middle Ordovician arthropod fauna (Trilobita, Ostracoda, Bradoriida) from the Lashkarak formation, eastern Alborz Mountains, northern Iran. *GFF*, *129*, 245–254. https://doi.org/10.1080/11035890701293245

Goldberg, S. L., Present, T. M., Finnegan, S., & Bergmann, K. D. (2021). A high-resolution record of early Paleozoic climate. *Proceedings of the National Academy of Sciences of the United States of America*, *118*(6). https://doi.org/10.1073/pnas.2013083118

Gradstein, F., & Ogg, J. (2020). The chronostratigraphic scale. In *Geologic time scale 2020* (pp. 21–32). Elsevier. https://doi.org/10.1016/b978-0-12-824360-2.00002-4

Grossman, E. L., & Joachimski, M. M. (2020). Oxygen isotope stratigraphy. In F. M.Gradstein, J. G.Ogg, M.Schmitz, & G.Ogg (Eds.), *Geologic time scale* (pp. 279–307). Elsevier. https://doi.org/10.1016/b978-0-12-824360-2.00010-3

Hallam, A. (1992). *Phanerozoic sea-level changes*. Columbia University Press.

Hansen, T., & Nielsen, A. T. (2003). Upper Arenig trilobite biostratigraphy and sea-level changes at Lynna River near Volkhov, Russia. *Bulletin of the Geological Society of Denmark*, *50*, 105–114. https://doi.org/10.37570/bgsd-2003-50-08

Haq, B. U., & Schutter, S. R. (2008). A chronology of Paleozoic sea-level changes. *Science*, *322*, 64–68. https://doi.org/10.1126/science.1161648

Holland, S. M. & Patskowsky, M. E. (1996). Sequence stratigraphy and long-term paleoceanographic change in the Middle and Upper Ordovician of the eastern United States In B. J.Witzke, G. A.Ludvigson, & J. E.Day (Eds.), *Paleozoic sequence stratigraphy: Views from the North American Craton*. Geological Society of America, Special Paper 306, pp. 117–130. https://doi.org/10.1130/0-8137-2306-x.117

Holland, S. M., & Patskowsky, M. E. (1998). Sequence stratigraphy and relative sea-level history of the Middle and Upper Ordovician of the Nashville Dome, Tennessee. *Journal of Sedimentary Research*, *68*, 684–699. https://doi.org/10.2110/jsr.68.684

Holmden, C., Creaser, R., Muehlenbachs, K., Leslie, S., & Bergstrom, S. (1998). Isotopic evidence for geochemical decoupling between ancient epeiric seas and bordering oceans: Implications for secular curves. *Geology*, *26*, 567–570. https://doi.org/10.1130/0091-7613(1998)026<0567:iefgdb>2.3.co;2

Huff, W. D., Bergström, S. M., & Kolata, D. R. (1992). Gigantic Ordovician volcanic ash fall in North America and Europe: Biological, tectonomagmatic, and event-stratigraphic significance. *Geology*, *20*(10), 875–878. https://doi.org/10.1130/0091-7613(1992)020<0875:govafi>2.3.co;2

Jaanusson, V. (1960). The Viruan (Middle Ordovician) of Öland. *Bulletin of the Geological Institutions of the University of Uppsala*, *38*, 207–288.

Jaanusson, V. (1961). Discontinuity surfaces in limestones. *Bulletin of the Geological Institutions of the University of Uppsala*, *40*(35), 221–241.

Jaanusson, V. (1973). Aspects of carbonate sedimentation in the Ordovician of Baltoscandia. *Lethaia*, *6*, 11–34. https://doi.org/10.1111/j.1502-3931.1973.tb00871.x

Jaanusson, V. (1976). Faunal dynamics in the Middle Ordovician (Viruan) of Balto-Scandia. In M. G.Bassett (Ed.), *The Ordovician System, Proceedings of a Palaeontological Association Symposium, Birmingham 1974* (pp. 301–326). University of Wales Press and National Museums of Wales.

Jaanusson, V. (1982a). Introduction to the Ordovician of Sweden. *Paper presented at the 4th International Symposium on the Ordovician System, Oslo*.

Jaanusson, V. (1982b). Ordovician in Västergötland. *Paper presented at the Field Excursion Guide. 4th International Symposium on the Ordovician System*.

Jaanusson, V. (1995). Confacies differentiation and upper Middle Ordovician correlation in the Baltoscandian Basin. *Proceedings of the Estonian Academy of Sciences: Geology*, *44*(2), 73–86. https://doi.org/10.3176/geol.1995.2.01

Jaffrés, J. B., Shields, G. A., & Wallmann, K. (2007). The oxygen isotope evolution of seawater: A critical review of a long-standing controversy and an improved geological water cycle model for the past 3.4 billion years. *Earth-Science Reviews*, *83*(1–2), 83–122.

Kaljo, D., Martma, T., & Saadre, T. (2007). Post-Hunnebergian Ordovician carbon isotope trend in Baltoscandia, its environmental implications and some similarities with that of Nevada. *Palaeogeography, Palaeoclimatology, Palaeoecology*, *245*(1–2), 138–155. https://doi.org/10.1016/j.palaeo.2006.02.020

Kanygin, A. V., Koren, T. N., Yadrenkina, A. G., Timokhin, A. V., Sychev, O. V., & Tolmacheva, T. Y. (2010). Ordovician of the Siberian platform. In S. C.Finney, & W. B. N.Berry (Eds.), *The Ordovician system* (Vol. 466, pp. 105–117). Geological Society of America Special Paper. https://doi.org/10.1130/2010.2466(07)

Kiipli, E., Kiipli, T., & Kallaste, T. (2009). Reconstruction of currents in the Mid-Ordovician–Early Silurian central Baltic Basin using geochemical and mineralogical indicators. *Geology*, *37*, 271–274. https://doi.org/10.1130/g25075a.1

Knoll, A. H., & Carroll, S. B. (1999). Early animal evolution: Emerging views from comparative biology and geology. *Science*, *284*(5423), 2129–2137. https://doi.org/10.1126/science.284.5423.2129

Korte, C., & Hesselbo, S. P. (2011). Shallow marine carbon and oxygen isotope and elemental records indicate icehouse-greenhouse cycles during the Early Jurassic. *Paleoceanography*, *26*(4), 18. https://doi.org/10.1029/2011PA002160

Korte, C., Jasper, T., Kozur, H. W., & Veizer, J. (2005). δ18O and δ13C of permian brachiopods: A record of seawater evolution and continental glaciation. *Palaeogeography, Palaeoclimatology, Palaeoecology*, *224*(4), 333–351. https://doi.org/10.1016/j.palaeo.2005.03.015

Korte, C., Thibault, N., Ullmann, C. V., Clemence, M.-E., Mette, W., Olsen, T. K., et al. (2017). Brachiopod biogeochemistry and isotope stratigraphy from the Rhaetian Eiberg section in Austria: Potentials and limitations. *Neues Jahrbuch für Geologie und Paläontologie - Abhandlungen*, *284*, 117–138. https://doi.org/10.1127/njgpa/2017/0651

Kröger, B., Franeck, F., & Rasmussen, C. M. Ø. (2019). The evolutionary dynamics of the early Palaeozoic marine biodiversity accumulation. *Proceedings of the Royal Society B*, *286*, 20191634.

Kroopnick, P., Margolis, S., & Wong, C. (1977). Paleoproductivity and ΣCO2-13C correlations in the atmosphere and oceans. *The fate of fossil fuel carbonates*. Office of Naval Research Symposium Series in Oceanography.

Lavoie, D. (1995). A late Ordovician high-energy temperate-water carbonate ramp, southern Québec, Canada: Implications for Late Ordovician oceanography. *Sedimentology*, *42*, 95–116. https://doi.org/10.1111/j.1365-3091.1995.tb01273.x

Le Hérissé, A., Al-Ruwaili, M., Miller, M., & Vecoli, M. (2007). Environmental changes reflected by palynomorphsinthe early Middle Ordovician Hanadir Member of the Qasim Formation, Saudi Arabia. *Revue de micropaleontology*, *50*, 3–16.

Lindskog, A., Costa, M. M., Rasmussen, C. M. Ø., Connelly, J. N., & Eriksson, M. E. (2017). Refined Ordovician timescale reveals no link between asteroid breakup and biodiversification. *Nature Communications*, *8*, 14066. https://doi.org/10.1038/ncomms14066

Lindskog, A., & Eriksson, M. E. (2017). Megascopic processes reflected in the microscopic realm: Sedimentary and biotic dynamics of the middle Ordovician "orthoceratite limestone" at Kinnekulle, Sweden. *GFF*, *139*(3), 163–183. https://doi.org/10.1080/11035897.2017.1291538

Lindskog, A., Eriksson, M. E., Bergström, S. M., & Young, S. A. (2019). Lower–Middle Ordovician carbon and oxygen isotope chemostratigraphy at Hällekis, Sweden: Implications for regional to global correlation and paleoenvironmental development. *Lethaia*, *52*(2), 204–219. https://doi.org/10.1111/let.12307

Lindström, M. (1963). Sedimentary folds and the development of limestone in the early Ordovician sea. *Sedimentology*, *2*, 243–292.

Lindström, M. (1971). *Lower Ordovician Conodonts of Europe* (Vol. 127, pp. 21–61). Geological Society of America Memoir.

Lindström, M. (1979). Diagenesis of Lower Ordovician hardgrounds in Sweden. *Geologica et Palaeontologica*, *13*, 9–30.

Lindström, M. (1984). The Ordovican climate based on the study of carbonate rocks. In D. L.Bruton (Ed.), *Aspects of the Ordovician system* (Vol. 295, pp. 81–88). Universitetforlaget.

Löfgren, A. (2000). Early to early Middle Ordovician conodont biostratigraphy of the Gillberga quarry, northern Öland, Sweden. *GFF*, *122*(4), 321–338.

Löfgren, A. (2003). Conodont faunas with Lenodus variabilis in the upper Arenigian to lower Llanvirnian of Sweden. *Acta Palaeontologica Polonica*, *48*(3), 417–436.

Männil, R. (1966). *Evolution of the Baltic Basin during the Ordovician*. Valgus Publishers.

McKenzie, N. R., Hughes, N. C., Gill, B. C., & Myrow, P. M. (2014). Plate tectonic influences on Neoproterozoic–early Paleozoic climate and animal evolution. *Geology*, *42*(2), 127–130. https://doi.org/10.1130/G34962.1

Miller, A. I., & Mao, S. (1995). Association of orogenic activity with the Ordovician radiation of marine life. *Geology*, *23*(4), 305–308. https://doi.org/10.1130/0091-7613(1995)023<0305:aooawt>2.3.co;2

Munnecke, A., Calner, M., Harper, D. A. T., & Servais, T. (2010). Ordovician and Silurian sea-water chemistry, sea-level, and climate: A synopsis. *Palaeogeography, Palaeoclimatology, Palaeoecology*, *296*, 389–413. https://doi.org/10.1016/j.palaeo.2010.08.001

Nielsen, A. T. (1995). Trilobite systematics, biostratigraphy and palaeoecology of the Lower Ordovician Komstad limestone and Huk formations, southern Scandinavia. *Fossils and Strata*, *38*, 1–374.

Nielsen, A. T. (2004). Ordovician sea level changes: A Baltoscandian perspective. In B. D.Webby, F.Paris, M. L.Droser, & I. C.Percival (Eds.), *The Great Ordovician biodiversification event* (pp. 84–93). Columbia University Press. https://doi.org/10.7312/webb12678-011

Nielsen, A. T. (2011). A re-calibrated revised sea-level curve for the Ordovician of Baltoscandia. *Cuadernos del Museo Geominero*, *14*, 399–401.

Panchuk, K., Holmden, C., & Kump, L. (2005). Sensitivity of the epeiric sea carbon isotope record to local-scale carbon cycle processes: Tales from the Mohawkian sea. *Palaeogeography, Palaeoclimatology, Palaeoecology*, *228*, 320–337. https://doi.org/10.1016/j.palaeo.2005.06.019

Pohl, A., Donnadieu, Y., Le Hir, G., Ladant, J.-B., Dumas, C., Alvarez-Solas, J., & Vandenbroucke, T. R. A. (2016). Glacial onset predatedLate Ordovician climate cooling. *Paleoceanography and Paleoclimatology*, *31*, 800–821. https://doi.org/10.1002/2016pa002928

Pope, M., & Read, J. F. (1998). Ordovician metre-scale cycles: Implications for climate and eustatic fluctuations in the central Appalachians during a global greenhouse, non-glacial to glacial transition. *Palaeogeography, Palaeoclimatology, Palaeoecology*, *138*, 27–42. https://doi.org/10.1016/s0031-0182(97)00130-2

Pörtner, H. O. (2001). Climate change and temperature-dependent biogeography: Oxygen limitation of thermal tolerance in animals. *Naturwissenschaften*, *88*, 137–146. https://doi.org/10.1007/S001140100216

Qing, H., & Veizer, J. (1994). Oxygen and carbon isotopic composition of Ordovician brachiopods: Implications for coeval seawater. *Geochimica et Cosmochimica Acta*, *58*(20), 4429–4442. https://doi.org/10.1016/0016-7037(94)90345-x

Quinton, P. C., Speir, L., Miller, J., Ethington, R., & MacLeod, K. G. (2018). Extreme heat in the Early Ordovician. *PALAIOS*, *33*, 353–360. https://doi.org/10.2110/palo.2018.031

Rasmussen, C. M. Ø., Kröger, B., Nielsen, M. L., & Colmenar, J. (2019). Cascading trend of early Paleozoic marine radiations paused by Late Ordovician mass extinctions. *Proceedings of the National Academy of Sciences of the United States of America*, *116*(15), 7207–7213. https://doi.org/10.1073/pnas.1821123116

Rasmussen, C. M. Ø., Nielsen, A. T., & Harper, D. A. T. (2009). Ecostratigraphical interpretation of lower Middle Ordovician East Baltic sections based on brachiopods. *Geological Magazine*, *146*(5), 717–731. https://doi.org/10.1017/s0016756809990148

Rasmussen, C. M. Ø., Ullmann, C. V., Jakobsen, K. G., Lindskog, A., Hansen, J., Hansen, T., et al. (2016). Onset of main Phanerozoic marine radiation sparked by emerging Mid Ordovician icehouse. *Scientific Reports*, *6*, 18884. https://doi.org/10.1038/srep18884

Rasmussen, J. A., & Stouge, S. (2018). Baltoscandian conodont biofacies fluctuations and their link to middle Ordovician (Darriwilian) global cooling. *Palaeontology*, *61*, 391–416. https://doi.org/10.1111/pala.12348

Rasmussen, J. A., Thibault, N., & Rasmussen, C. M. Ø. (2021). Middle Ordovician astrochronology decouples asteroid breakup from glacially-induced biotic radiations. *Nature Communications*, *12*, 6430. https://doi.org/10.1038/s41467-021-26396-4

Ross, C. A., & Ross, J. R. P. (1995). North American Ordovician depositional sequences and correlations. In J.Cooper, M. L.Droser, & S.Finney (Eds.), *Ordovician Odyssey. 7th Las Vegas, The Pacific Section Society of Sedimentary Geology (SEPM)*, pp. 309–313.

Ross, J. R. P., & Ross, C. A. (1992). Ordovician sea-level fluctuations. In B. D.Webby, & J. R.Laurie (Eds.), *Global Perspectives on Ordovician Geology. Proceedings of the 6th International Symposium on the Ordovician System* (pp. 327–335). Balkema.

Saltzman, M. M., & Thomas, E. (2012). Chapter 11 – Carbon isotope stratigraphy. In F. M.Gradstein, J. G.Ogg, M.Schmitz, & G.Ogg (Eds.), *The geologic time scale 2012* (pp. 207–232). Elsevier BV. https://doi.org/10.1016/b978-0-444-59425-9.00011-1

Saltzman, M. R., & Edwards, C. T. (2017). Gradients in the carbon isotopic composition of Ordovician shallow water carbonates: A potential pitfall in estimates of ancient CO_2 and O_2. *Earth and Planetary Science Letters*, *464*, 46–54. https://doi.org/10.1016/j.epsl.2017.02.011

Saltzman, M. R., & Young, S. A. (2005). Long-lived glaciation in the Late Ordovician? Isotopic and sequence-stratigraphic evidence from western Laurentia. *Geology*, *33*, 109–112. https://doi.org/10.1130/g21219.1

Schmitz, B., Bergström, S. M., & Xiaofeng, W. (2010). The middle Darriwilian (Ordovician) ^{13}C excursion (MDICE) discovered in the Yangtze platform succession in China: Implications of its first recorded occurrences outside Baltoscandia. *Journal of the Geological Society*, *167*, 249–259. https://doi.org/10.1144/0016-76492009-080

Schmitz, B., Farley, K. A., Goderis, S., Heck, P. R., Bergström, S. M., Boschi, S., et al. (2019). An extraterrestrial trigger for the mid-Ordovician ice age: Dust from the breakup of the L-chondrite parent body. *Science Advances*, *5*, eaax4184. https://doi.org/10.1126/sciadv.aax4184

Shields, G. A., Carden, G. A. F., Veizer, J., Meidla, T., Rong, J.-y., & Li, R.-y. (2003). Sr, C, and O isotope geochemistry of Ordovician brachiopods: A major isotopic event around the Middle–Late Ordovician transition. *Geochimica et Cosmochimica Acta*, *67*(11), 2005–2025. https://doi.org/10.1016/s0016-7037(02)01116-x

Steuber, T., & Veizer, J. (2002). Phanerozoic record of plate tectonic control of seawater chemistry and carbonate sedimentation. *Geology*, *30*(12), 1223–1126. https://doi.org/10.1130/0091-7613(2002)030<1123:proptc>2.0.co;2

Stouge, S. (2004). Ordovician siliciclastics and carbonates of Öland, Sweden, 91–111. Paper Presented at the Annual Meeting of IGCP Project No 503. Erlangen.

Stouge, S., & Bagnoli, G. (1990). Lower Ordovician (Volkhovian–Kundan) conodonts from Hagudden, northern Öland, Sweden. *Paleontographia Italica*, *77*, 1–54.

Stouge, S., & Bagnoli, G. (2014). Timing of the deposition of the remarkable 'green unit' (early Middle Ordovician) on Öland, Sweden. *Paper presented at the 4th Annual Meeting of IGCP 591 – Abstracts and Field Guide Tartu, Estonia.*

Stouge, S., Bagnoli, G., & Rasmussen, J. A. (2020). Late Cambrian (Furongian) to mid-Ordovician euconodont events on Baltica: Invasions and immigrations. *Palaegeography, Palaeoclimatology, Palaeoecology*, *549*, 109151. https://doi.org/10.1016/j.palaeo.2019.04.007

Swart, P. K. J. S. (2015). The geochemistry of carbonate diagenesis. *The past, present and future*, *62*(5), 1233–1304. https://doi.org/10.1111/sed.12205

Takayanagi, H., Asami, R., Abe, O., Miyajima, T., Kitagawa, H., Sasaki, K., & Iryu, Y. (2013). Intraspecific variations in carbon-isotope and oxygen-isotope compositions of a brachiopod *Basiliola lucida* collected off Okinawa-jima, southwestern Japan. *Geochimica et Cosmochimica Acta*, *115*, 115–136. https://doi.org/10.1016/j.gca.2013.03.026

Takayanagi, H., Asami, R., Otake, T., Abe, O., Miyajima, T., Kitagawa, H., & Iryu, Y. (2015). Quantitative analysis of intraspecific variations in the carbon and oxygen isotope compositions of the modern cool-temperate brachiopod *Terebratulina crossei*. *Geochimica et Cosmochimica Acta*, *170*, 301–320. https://doi.org/10.1016/j.gca.2015.08.006

Tjernvik, T. E. (1956). On the Early Ordovician of Sweden. Stratigraphy and Fauna. *Bulletin of the Geological Institution of the University of Upsala*. *36*, 107–284.

Torsvik, T. H., & Cocks, L. (2019). The integration of palaeomagnetism, the geological record and mantle tomography in the location of ancient continents. *Geological Magazine*, *156*, 242–260. https://doi.org/10.1017/s001675681700098x

Torsvik, T. H., & Cocks, L. R. M. (2016). Ordovician. In *Earth history and paleogeography* (pp. 101–123). Cambridge University Press.

Torsvik, T. H., & Rehnström, E. (2003). The Tornquist Sea and Baltica – Avalonia docking. *Tectonophysics*, *362*, 67–82. https://doi.org/10.1016/s0040-1951(02)00631-5

Torsvik, T. H., Smethurst, M. A., Voo, R. V. D., Trench, A., Abrahamsen, N., & Halvorsen, E. (1992). Baltica. A synopsis of Vendian – Permian palaeomagnetic data and their palaeotectonic implications. *Earth-Science Reviews*, *33*, 133–152. https://doi.org/10.1016/0012-8252(92)90023-m

Torsvik, T. H., Van der Voo, R., Preeden, U., MacNiocaill, C., Steinberger, B., Doubrovine, P. V., et al. (2012). Phanerozoic polar wander, palaeogeography and dynamics. *Earth-Science Reviews*, *114*, 325–368. https://doi.org/10.1016/j.earscirev.2012.06.007

Trotter, J. A., Williams, I. S., Barnes, C. R., Lécuyer, C., & Nicoll, R. S. (2008). Did cooling oceans trigger Ordovician biodiversification? Evidence from conodonts thermometry. *Science*, *321*, 550–554. https://doi.org/10.1126/science.1155814

Tullborg, E.-L., Larsson, S. A., Björklund, L., Stigh, J., & Samuelsson, L. (1995). Thermal evidence of Caledonide foreland, molasse sedimentation in Fennoscandia. *Swedish Nuclear Fuel and Waste Management Company Technical Report*, *95–18*, 47.

Turner, B. R., Armstrong, H. A., & Holt, P. (2011). Visions of ice sheets in the early Ordovician greenhouse world: Evidence from the Peninsula Formation, Cape Peninsula, South Africa. *Sedimentary Geology*, *236*, 226–238. https://doi.org/10.1016/j.sedgeo.2011.01.009

Turner, B. R., Armstrong, H. A., Wilson, C. R., & Makhlouf, I. M. (2012). High frequency eustatic sea-level changes during the Middle to early Late Ordovician of southern Jordan: Indirect evidence for a Darriwilian Ice Age in Gondwana. *Sedimentary Geology*, *251*(252), 34–48. https://doi.org/10.1016/j.sedgeo.2012.01.002

Ullmann, C., Boyle, R., Duarte, L., Hesselbo, S. P., Kasemann, S. A., Klein, T., et al. (2020). Warm afterglow from the Toarcian Oceanic Anoxic Event drives the success of deep-adapted brachiopods. *Scientific Reports*, *10*, 6549.

Ullmann, C. V., Campbell, H. J., Frei, R., Hesselbo, S. P., Pogge von Strandmann, P. A. E., & Korte, C. (2013). Partial diagenetic overprint of Late Jurassic belemnites from New Zealand: Implications for the preservation of δ^7Li values in calcite fossils. *Geochimica et Cosmochimica Acta*, *120*, 80–96. https://doi.org/10.1016/j.gca.2013.06.029

Ullmann, C. V., Frei, R., Korte, C., & Lüter, C. (2017). Element/Ca, C and O isotope ratios in modern brachiopods: Species-specific signals of biomineralization. *Chemical Geology*, *460*, 15–24. https://doi.org/10.1016/j.chemgeo.2017.03.034

Valentine, J. W., & Moores, E. W. (1970). Plate-tectonic regulation of faunal diversity and sea level: A model. *Nature*, *228*, 657–659. https://doi.org/10.1038/228657a0

Vandenbroucke, T. R. A., Armstrong, H. A., Williams, M., Paris, F., Sabbe, K., Zalasiewicz, J. A., & Verniers, J. (2010). Epipelagic chitinozoan biotopes map a steep latitudinal temperature gradient for earliest Late Ordovician seas: Implications for a cooling Late Ordovician climate. *Palaeogeography, Palaeoclimatology, Palaeoecology*, *294*(3–4), 202–219. https://doi.org/10.1016/j.palaeo.2009.11.026

Vandenbroucke, T. R. A., Armstrong, H. A., Williams, M., Paris, F., Zalasiewicz, J., Sabbe, K., et al. (2010). Polar front shift and atmospheric CO_2 during the glacial maximum of the Early Paleozoic Icehouse. *Proceedings of the National Academy of Sciences of the United States of America*, *107*(34), 14983–14986. https://doi.org/10.1073/pnas.1003220107

van de Schootbrugge, B., Föllmi, K. B., Bulot, L. G., & Burns, S. J. (2000). Paleoceanographic changes during the early Cretaceous (Valanginian–Hauterivian): Evidence from oxygen and carbon stable isotopes. *Earth and Planetary Science Letters*, *181*(1–2), 15–31. https://doi.org/10.1016/s0012-821x(00)00194-1

van Wamel, W. A. (1974). Conodont biostratigraphy of the Upper Cambrian and Lower Ordovician of North-Western Öland, South-Eastern Sweden. *Utrecht Micropaleontological Bulletins*. (Vol. 10).

Veizer, J., Ala, D., Azmy, K., Bruckschen, P., Buhl, D., Bruhn, F., et al. (1999). 87Sr/86Sr, δ13C and δ18O evolution of Phanerozoic seawater. *Chemical Geology*, *161*, 92–104. https://doi.org/10.1016/s0009-2541(99)00081-9

Veizer, J., Godderis, Y., & Francois, L. M. (2000). Evidence for decoupling of atmospheric CO_2 and global climate during the Phanerozoic eon. *Nature*, *408*, 698–701. https://doi.org/10.1038/35047044

Veizer, J., & Prokoph, A. (2015). Temperatures and oxygen isotopic composition of Phanerozoic oceans. *Earth-Science Reviews*, *146*, 92–104. https://doi.org/10.1016/j.earscirev.2015.03.008

Verard, C., & Veizer, J. (2019). On plate tectonics and ocean temperatures. *Geology*, *47*(9), 881–885. https://doi.org/10.1130/g46376.1

Wu, R., Calner, M., & Lehnert, O. (2017). Integrated conodont biostratigraphy and carbon isotope chemostratigraphy in the Lower–Middle Ordovician of southern Sweden reveals a complete record of the MDICE. *Geological Magazine*, *154*(2), 334–353. https://doi.org/10.1017/s0016756816000017

Young, S. A., Gill, B. C., Edwards, C. T., Saltzman, M. R., & Leslie, S. A. (2016). Middle–Late Ordovician (Darriwilian–Sandbian) decoupling of global sulfur and carbon cycles: Isotopic evidence from eastern and southern Laurentia. *Palaeogeography, Palaeoclimatology, Palaeoecology*, *458*, 118–132. https://doi.org/10.1016/j.palaeo.2015.09.040

Zaffos, A., Finnegan, S., & Peters, S. E. (2017). Plate tectonic regulation of global marine animal diversity. *Proceedings of the National Academy of sSciences of the United States of America*, *114*(22), 5653–5658. https://doi.org/10.1073/pnas.1702297114

Zhan, R., Jin, J., & Chen, P. (2007). Brachiopod diversification during the Early-Mid Ordovician: An example from the Dawan formation, Yichang area, central China. *Canadian Journal of Earth Sciences*, *44*(1), 9–24. https://doi.org/10.1139/e06-069

Zhang, J. (1998). Middle Ordovician conodonts from the Atlantic Faunal Region and the evolution of key conodont genera. *Meddelanden från Stockholms universitets institution för geologi och geokem*, *298*, 1101–1599.

References From the Supporting Information

Brand, U., Logan, A., Hiller, N., & Richardson, J. (2003). Geochemistry of modern brachiopods: Applications and implications for oceanography and paleoceanography. *Chemical Geology*, *198*, 305–334. https://doi.org/10.1016/s0009-2541(03)00032-9

Brand, U., & Veizer, J. (1980). Chemical diagenesis of a multicomponent carbonate system; 1, Trace elements. *Journal of Sedimentary Research*, *50*(4), 1219–1236. https://doi.org/10.1306/212f7bb7-2b24-11d7-8648000102c1865d

Brand, U., & Veizer, J. (1981). Chemical diagenesis of a multicomponent carbonate system – 2: Stable isotopes. *Journal of Sedimentary Petrology*, *51*(3), 987–997.

Korte, C., Jones, P. J., Brand, U., Mertmann, D., & Veizer, J. (2008). Oxygen isotope values from high-latitudes: Clues for Permian sea-surface temperature gradients and Late Palaeozoic deglaciation. *Palaeogeography, Palaeoclimatology, Palaeoecology*, *269*, 1–16. https://doi.org/10.1016/j.palaeo.2008.06.012

Rasmussen, B. W., Rasmussen, J. A., & Nielsen, A. T. (2017). Biostratigraphy of the Furongian (upper Cambrian) Alum Shale Formation at Degerhamn, Öland, Sweden. *GFF*, *139*(2), 92–118. https://doi.org/10.1080/11035897.2016.1276099

Schobben, M., Ullmann, C. V., Leda, L., Korn, D., Struck, U., Reimold, W. U., et al. (2016). Discerning primary versus diagenetic signals in carbonate carbon and oxygen isotope records: An example from the Permian–Triassic boundary of Iran. *Chemical Geology*, *422*, 94–107. https://doi.org/10.1016/j.chemgeo.2015.12.013

Terfelt, F., Eriksson, M. E., & Schmitz, B. (2014). The Cambrian–Ordovician transition in dysoxic facies in Baltica—Diverse faunas and carbon isotope anomalies. *Palaeogeography, Palaeoclimatology, Palaeoecology*, *394*, 59–73. https://doi.org/10.1016/j.palaeo.2013.11.021

Ullmann, C. V., & Korte, C. (2015). Diagenetic alteration in low-Mg calcite from macrofossils: A review. *Geological Quarterly*, *59*(1), 3–20. https://doi.org/10.7306/gq.1217